Special Collection

Electroless Plating of Metal Nanomaterials

Falk Muench*[a]

Dedicated to Prof. Wolfgang Ensinger for providing me the opportunity to freely choose and develop my research focus, to my family, and the most successful of my experiments-my children.

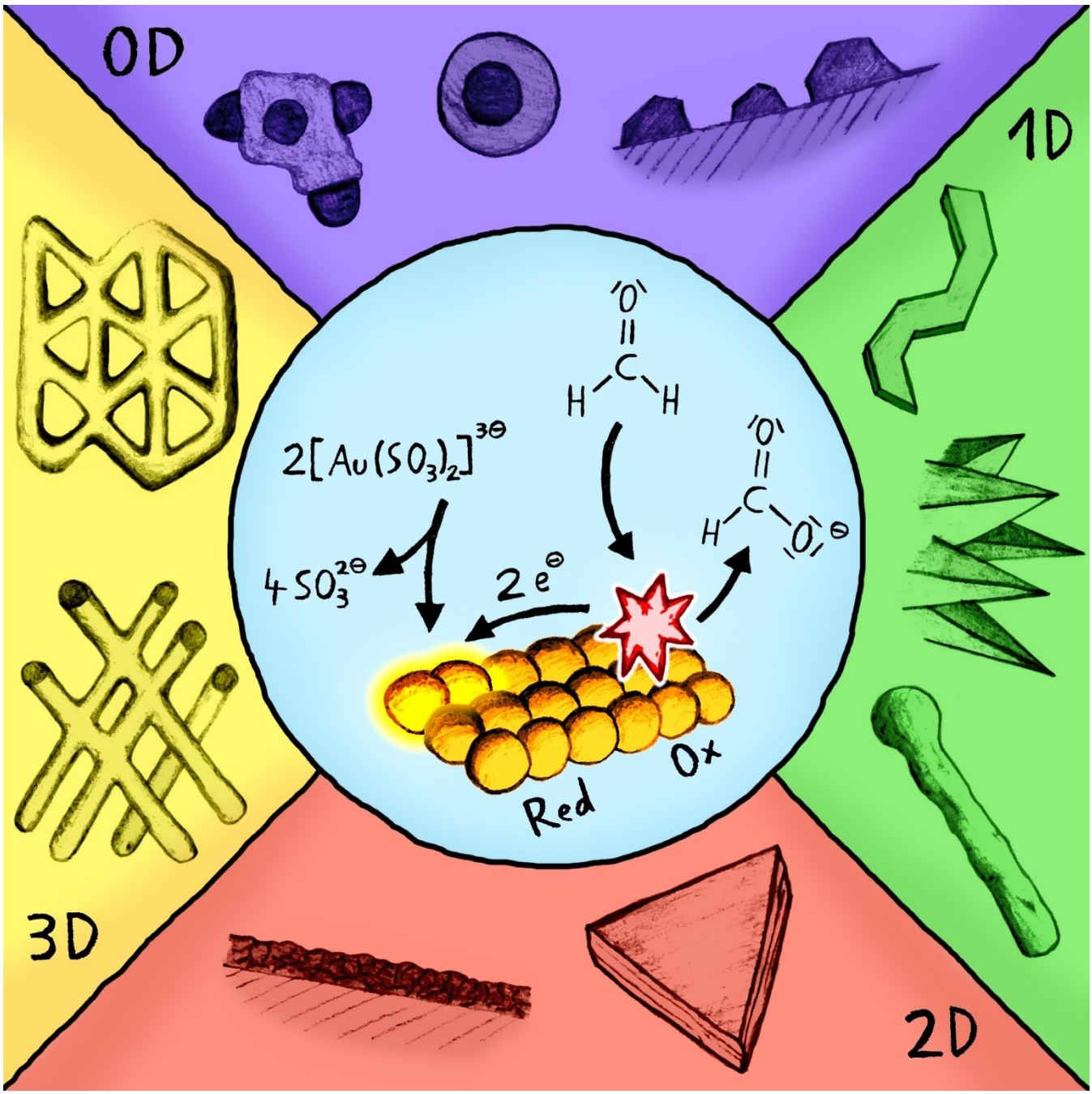

Electroless plating is commonly associated with metallizing macroscopic work pieces, but also represents a surprisingly powerful nanomanufacturing tool. This review details the technique's use for creating nanomaterials of arbitrary dimensionality, ranging from nanoparticles over nanotubes, nanowires, and ultrathin films to nanostructured lattices, focusing on the solution chemistry and mechanistic aspects. The synthesis of defined nanostructures serves as overarching perspective, which is enriched by drawing connections to and insights from related fields. Strategies for controlling the size, shape, crystallinity, porosity, composition, and arrangement of electrolessly plated nanostructures are outlined, including templating (which harnesses the method's exceptional conformality to guide and limit deposit formation), the complementary approach of selective growth, tailored seeding, and bath design. Being able to strike convincing compromises between material quality and ease of preparation, electroless nanoplating has a distinct potential to facilitate the application of metal nanomaterials.

1. Introduction

Nanotechnology deals with the creation and implementation of materials possessing features approximately seven to nine orders of magnitude smaller than a meter. If a human took the role of a rather big nanoparticle and searched for an enlarged structure of corresponding scale, it could look at nothing less than the earth, whose diameter provides a comparable size ratio. Assembling matter at such tiny length scales is no doubt a challenging task, but successful attempts are rewarded with materials possessing huge surface-to-volume ratios, altered properties and previously unobserved functionality, enabling the construction of miniaturized, more efficient, or entirely novel devices. A completely realized nanotechnology – granting full control over the positioning of single atoms as the smallest building blocks of condensed matter – could be interpreted as the ultimate form of materials science.

While synthetic perfection[1] remains an as important as elusive goal in itself, one must factor in trade-offs between precision and materials performance on the one hand, and process efficiency on the other. As the properties of nano-objects strongly depend on their shape, size, composition, internal structure, and surface chemistry,[2] techniques providing extensive control over these parameters are in high demand. However, precise techniques tend to rely on complex instrumentation, exotic educts, and special environments (*e.g.*, vacuum, protective gas, cleanrooms), and are frequently held back by low yields and time-consuming procedures. In contrast, the broad-scale implementation of nanomaterials requires cost-efficient, robust synthetic approaches of high throughput, particularly in industrial context.[3]

Considering metal nanomaterials, solution-based methods like galvanic displacement,[4] reductive precipitation,[5] electroless plating or electrodeposition[6] regularly achieve convincing compromises between synthetic precision and feasibility. Sophisticated wet-chemical protocols can create exquisite nanostructures such as monodisperse metal nanocrystals, epitaxially overcoated with shells of a secondary metal, just a couple of atomic layers thick.[7] During the advent of nanoscience, techniques like electrodeposition have been firmly established as standard tools for producing metal nanomaterials,[8] and publications simultaneously covering the topics "nano" and "electrodeposition" have gained noticeable momentum since the early 2000s (Figure 1). Throughout this time period, electrodeposition papers have remained about seven times more frequent than their electroless plating counterparts.

The extent of this gap could appear surprising, considering the close relationship of both methods[6] and the beneficial characteristics of electroless plating, which deposits conformal metal films by surface-selective chemical reduction.[6,9,10] Electroless plating offers a route towards metal nanomaterials through simple wet-chemical means, by immersing suitable samples into aqueous solutions for defined amounts of time. Not reliant on electrical contacting, the method is almost absurdly flexible regarding the substrate to be metallized, irrespective of its state of matter, composition, and morphology. Suitable substrates include gas nano-bubbles,[11] emulsified droplets,[12] dispersed nanoparticles,[13] artful three-dimensional lattices,[14] diatom shells,[15] spirulina filaments,[16] laser-written microfluidic channels[17] and block copolymer templates.[18] This astonishing flexibility allows constructing manifold nanomaterials, which range from quasi-zero-dimensional nanoparticles[13] over

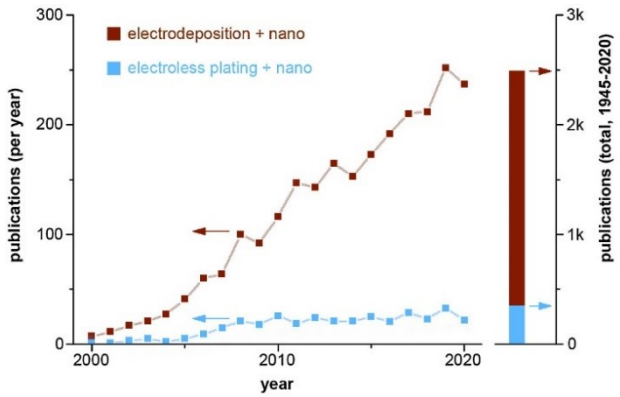

Figure 1. Number of published papers simultaneously covering "nano" and either "electroless plating" or "electrodeposition" (Web of Science Core Collection topic search, accessed on March 9th, 2021).

[a] *Dr. F. Muench*
Department of Materials and Earth Sciences
Technical University of Darmstadt
Alarich-Weiss-Straße 2, 64287 Darmstadt, Germany
E-mail: muench@ma.tu-darmstadt.de

An invited contribution to a Special Collection dedicated to Electrochemistry 2020: At the Interface between Chemistry and Physics

nanowires[19] and nanoplates[20] to monolithic nanostructured materials.[14]

Electroless plating is a mature technology which can look back at an extended history and a decade-long industrial implementation.[9,21] The method was accidentally re-discovered and promoted[22,23] by Brenner and Riddel in 1946,[24] but the concept can be traced back to the seminal work of Wurtz, who described nickel plating as early as 1844.[25] It is understandable that the use of a well-established surface finishing technique, which is less associated with high technology, more with bulky products and down-to-earth applications such as corrosion protection, can be met with hesitation, as it does not constitute an ideal buzzword for selling cutting-edge science. One might even need to justify its use in perfectly viable scenarios, as evident in the following quote, which stems from a study applying electroless plating as enabling technology to create chiral plasmonic crystals: "We note that standard deposition methods such as sputter coating or vacuum evaporation were unsuitable for metal coating due to self-shadowing of the complex 3D geometry".[26]

While the ties between the electroless plating and nanomaterials communities can be strengthened, there is no shortage of common themes. Conventional electroless plating is dominated by nickel deposition, but the method can deposit many late transition metals prevalent in nanomaterial applications. Classical processes yield compact, smooth, bright, and thick metal films (at least from a nanomaterials perspective), which typically serve as protective or conductive coatings.[9,27] But the method can also create anisotropic structures, patterned and roughened coatings for application in catalysis, sensing or plasmonics. To fully harness the nanomanufacturing potential of electroless plating, it is important to overcome its existing structural and compositional limitations, and to adapt its process characteristics to new requirements.

The present review aims at raising the awareness of the potential – both realized and untapped – of electroless plating from the specific viewpoint of its ongoing development as a nanomanufacturing tool. It adopts an overarching synthetic narrative, which includes a tutorial-level introduction to the mechanistic foundations and discusses in detail the intricacies of the bath chemistry and of controlling the composition, shape, crystallinity, and distribution of the plated nanomaterials, which act as key parameters for tailoring their functionality. The history of electroless plating, which already has been succinctly described,[21–23] is omitted. Nanocomposite plating,[27] which is concerned with the codeposition of nanoscale additives (typically to enhance properties in established applications, *e.g.*, increasing the coating hardness or friction coefficient), is excluded as well. The electroless plating of interconnects in micro-/nanoelectronics is already excellently covered by dedicated reviews,[21,28] to which the reader is referred.

Following the synthesis focus, application aspects are interwoven with mechanistic arguments rather than discussed separately. My intent is to outline the advantages, disadvantages, challenges, and potential development paths of nanoscale electroless plating by providing a consolidated source of information. While no single method solves all synthetic problems, electroless plating offers a surprisingly versatile route towards metal nanostructures. From first-hand experience, I can also confirm that it is a rather quirky technique. If this review can spark curiosity, encourage researchers to play and perhaps even help them with tackling some of the method's difficulties, I would be a happy chemist.

After studying chemistry in Ulm and Marburg, Falk Muench received his Ph.D. degree from the Technical University of Darmstadt in 2013, followed by research in the groups of Prof. W. Ensinger (Technical University of Darmstadt) and Prof. I. Rubinstein (Weizmann Institute of Science). He is developing solution deposition reactions for functional coatings, focussing on anisotropic metal nanostructures, electrochemistry, and heterogeneous catalysis. From the beginning, he fell for the intricacies of electroless plating and nanotechnology, which reliably relieve his itch for creative chemistry.

2. The Mechanism of Electroless Plating

Electroless plating represents a reaction class which utilizes the heterogeneously autocatalyzed conversion of metastable redox pairs – formed by dissolved reducing agents and metal complexes – for achieving conformal metallization.[6,9,10] The overall process can be summarized as two coupled redox reactions: The oxidation of a reducing agent, and the reduction of a metal complex (Figure 2A). Thus, the method can be interpreted in the framework of mixed potential theory,[29] although factors such as interdependent or diffusion-controlled partial reactions can impede such an analysis.[30] Also, its fundamental properties can be interrogated in electrochemical experiments.[9,29–31]

Electroless plating starts with a metastable redox pair and ends with elemental metal and oxidized reducer. Various processes contribute to the activation energy barrier separating these boundary states (*e.g.*, reducer conversion, metal complex reduction, rearrangement and shedding of ligands, adatom formation, migration, and integration into the deposit lattice). Three main reaction trajectories lead to the end state (Figure 2B). The apparent activation energies for electroless plating reactions depend on the specific system. Typical values range from 74.1 $kJ\,mol^{-1}$ for Ni plating with hypophosphite to 49.0 $kJ\,mol^{-1}$ for Cu plating with formaldehyde.[31] While reducer conversion often represents the rate-determining step,[30] the activation energies of anodic reducer oxidation are typically below those of the net plating reaction, probably because the former does not account for additional relevant barriers (metal ion stabilization by complexation, cathodic metal deposition).[31] Individual reaction steps and intermediate energies can be resolved with theoretical bonding studies.[32] Energy differences between the competing reaction pathways are difficult to quantify, since these involve complicating factors such as

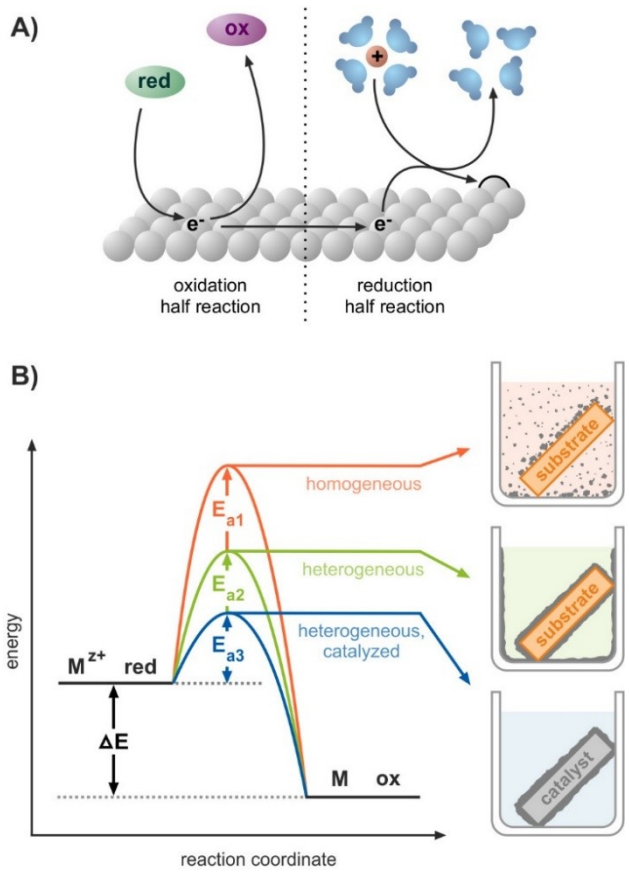

Figure 2. A) Reaction scheme exemplifying the coupled partial reactions of electroless plating with the reduction of a singly charged aquo complex. B) Reaction path showing three routes towards metal formation.

nucleation steps, interfacial interactions, and transitioning mechanisms.

A homogeneous reaction in the bulk solution results in homogeneous nucleation and particle precipitation (Figure 2B, orange route). This behavior is typical for too reactive plating bath formulations,[33] but can also be observed in overaged solutions. Due to the nucleation barrier (which can be estimated using classical nucleation theory)[34] and missing catalytic action, this pathway is associated with high activation energies, which provide the basis for suppressing uncontrolled metal reduction.

Metal atoms forming in the solution can also deposit on interfaces which lower the nucleation barrier (Figure 2B, green route). One famous example is Tollens' test, in which an alkaline, ammoniac solution of Ag(I) responds to the addition of reducing aldehydes with the spontaneous formation of silver mirrors and/or powders. In this deposition mode, quite arbitrary, noncatalytic surfaces can be coated with metal films,[35–37] which often comes at the cost of reduced stability and selectivity: Unwanted surfaces can be coated alongside the sample (*e.g.*, the reaction vessel), and the localized deposition of metal patterns is impeded. Deposition-promoting and -inhibiting surface chemistries provide a limited way of maintaining selectivity even in the case of unspecific plating baths. The attachment or nucleation of metal particles on noncatalytic surfaces, which initiates autocatalytic metal deposition on undesired areas, can be suppressed by minimizing electrostatic interactions between solution species and the substrate. Inversely, seeding and metallization generally are favored on polar, hydrophilic surfaces.[38] Such differences in reactivity can be used to direct metallization: Negatively charged silica particles could be metallized even without a dedicated seeding step (likely by attracting oppositely charged Ag(I) ions, which are then reduced *in situ)*, while plating did not proceed on the hydrophobic polypropylene reaction vessel.[39]

In its archetypical mode, electroless plating only proceeds at catalytic interfaces which considerably lower the activation energy, channeling metal deposition into this path (Figure 2B, blue route). As the product of the reaction (the deposited metal) is driving the redox reaction (and thus its own formation), electroless plating reactions are considered autocatalytic, and metal deposits grow continuously. The autonomous nature of the reaction results in an excellent degree of conformality.

Substrate-selective electroless plating represents a twisted version of this standard reactivity. Here, the catalytic substrate but not the deposit is capable of activating metallization, stopping the process once a coating is formed.[40] Self-limiting reactions like underpotential or atomic layer deposition create ultrathin conformal layers by stalling uncontrolled material accumulation. Considering the synthetic value of this concept, it appears highly worthwhile to deploy self-terminating strategies in electroless nanoplating as well.[41,42]

Electroless plating can be understood as member of a family of solution-based techniques which produce elemental metal by reducing dissolved metal ions (Figure 3). It could be interpreted as a variant of electrodeposition in which the electrons for reduction are not externally supplied, but produced *in situ* by the catalytic oxidation of the reducing agent. Electroless plating also bears striking similarity to the synthesis of metal nanoparticle colloids by chemical reduction. This is particularly true for autocatalyzed, seed-mediated nanoparticle syntheses,[5,43,44] which could be classified as electroless plating reactions applied to dispersed catalyst particles instead of solid work pieces. While such reactions can be more forgiving in terms of metastability (the presence of evenly distributed sites for metal deposition can help staying below the concentration threshold for spontaneous homogeneous nucleation),[34] the underlying reaction mechanism is identical. Given this close relationship, it is not astounding that electroless plating is well-suited for creating materials which are typically obtained by seed-mediated colloidal growth (*e.g.*, bimetallic nanoparticles,[13,45] anisotropic nanostructures).[19,20,46]

To avoid confusion, it should be noted that electroless deposition and electroless plating are often used interchangeably, and that methods such as galvanic displacement are frequently termed as electroless deposition. While galvanic displacement resembles electroless plating in that it does not require an external current, it deviates in key mechanistic aspects (no autocatalysis, reaction not carried by a dissolved reducer).

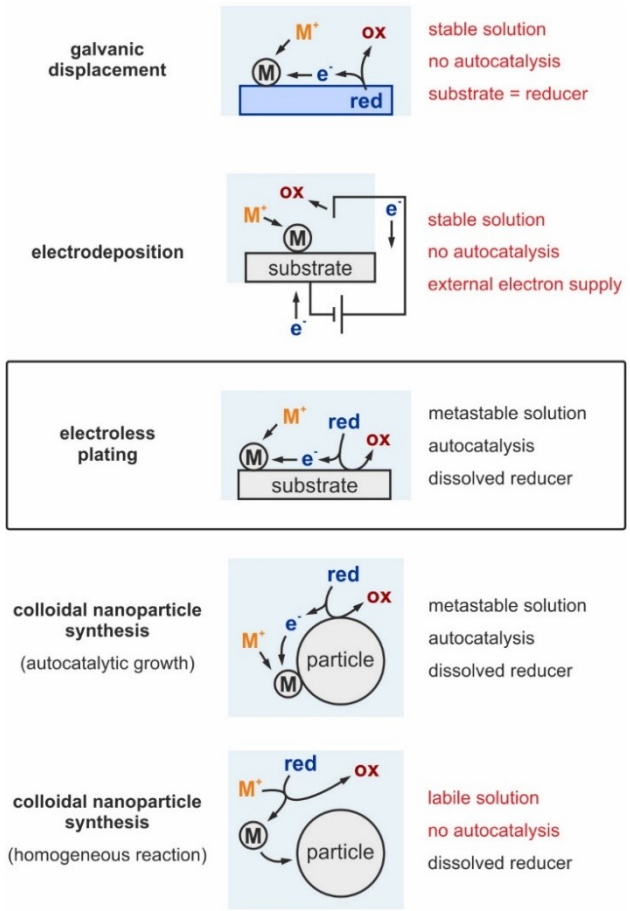

Figure 3. Schematic depictions of different solution-based methods utilizing the reduction of metal complexes. The reaction characteristics shown on the right are color-coded to indicate whether they match (black) or differ from (red) those of electroless plating.

3. Plating Bath Chemistry

At the heart of each electroless plating bath lies the simple combination of at least one metal complex and a reducing agent. However, auxiliary components such as stabilizers, buffers or surfactants are often needed, individual reagents regularly take on multiple roles, and the solution composition and reactivity are subject to spatiotemporal changes (*e.g.*, local pH variation, consumption of educts, formation of byproducts, aging, change of catalytic interfaces), considerably complicating the matter. As the bath chemistry defines the overall reactivity – including vital factors such as the solution lifetime, plating rate, deposit composition and morphology[9,27,47] – it is important to master and keep track of it, both for trouble-shooting experiments and for developing novel plating protocols. Detailed summaries of classical bath formulations and plating conditions can be found in the literature.[6,9,27,47,48]

To function properly, plating baths must operate at the edge of decomposition, and this chemical metastability is a fine line to walk. Contaminations or aging can trigger the plating out of metal powder, making cleanliness and care imperative. For laboratory purposes, aging issues can be mitigated by only working with freshly prepared plating baths. Individually stable components such as solutions containing the metal complex and the reducing agent can be stored separately and conveniently combined to assemble the final plating bath just before starting the reaction. While the method is quite straightforward to scale up, using small baths and discarding them after single use is much simpler than ensuring long bath lifetimes, monitoring, and replenishing the bath composition, and devising setups for continuous plating, particle filtration, controlled stirring, sample positioning, and wastewater management.[9] Solving such issues for nanomaterial plating baths is rarely performed[49] and might be a more technology-oriented and menial task. Regardless, it is a particularly important one for transitioning these techniques to mass production.

The facility and flexibility of electroless plating is especially useful when working on laboratory and prototyping scales, and in conjunction with 3D printing.[17,38,50,51] Due to the reliance on chemical reducers and the more involved bath management, electroless plating reactions are more expensive than comparable electrodepositions.

Using electroless plating for creating nanomaterials also has a unique advantage over classical applications. In the latter, it is paramount to achieve high plating rates to keep processing times reasonably short (typical rates range from several up to few tens of μm per hour,[9,47] with common target thicknesses of some tens of μm). Only needing to obtain nanoscale deposits completely overturns the reaction requirements. Low plating rates not only become tolerable, but even advantageous: Depositing nanostructures over the course of minutes (rather than seconds) is more reliable, particularly in scenarios in which the reaction cannot be terminated instantaneously (*e.g.*, plating dispersed powders).

In such an altered design space, new synthetic targets can take center stage, such as precise structural control, an aim of utmost nanotechnological importance. While the established use of electroless coatings in corrosion protection clearly discourages porous deposits, such morphologies can be rewarding in, *e.g.*, catalytic applications (see section 4.8). Between bath stability and reactivity, a loose inverse correlation exists (which is reflected, *e.g.*, in the plating rate). Being able to trade-off deposition speed for an increased solution lifetime is invaluable for depositing metals like silver, whose baths are notoriously unstable (Ref. [9], p. 442), but can be turned into dependable nanomanufacturing tools by tuning down their reactivity.[52–56] Plating rates in the range of tens to hundreds of nanometers per hour are perfectly adequate for depositing nanomaterials in convenient time frames (*e.g.*, functional silver nanoparticle coatings can be plated within minutes).[55]

3.1. Solvent

Electroless plating is typically performed in the desirable[57] solvent water, but it is not restricted to it. Surface-selective chemical metal depositions have also been achieved in organic solvents,[36,39,58] ionic liquids[59] and supercritical fluids.[60] Dis-

advantages posed by the use of organics and pressurized isochoric processes can be offset by unique benefits: Supercritical media offer rapid diffusion, high deposition rates and excellent conformality,[60] while nonaqueous solvents enable the deposition of extremely oxophilic metals such as aluminum[58,59] and show interesting reactivities (*e.g.*, nanofilm deposition on non-catalytic surfaces).[36,39] Organic solvents can simultaneously act as the reducer,[36] similar to colloidal approaches like polyol reactions.[61] While moving away from aqueous environments and gentle reaction conditions sacrifices key advantages of electroless plating (and thus should be considered with care), such measures open up considerable room for exploring new plating concepts.

3.2. Metal Complex

The metal complex constitutes the deposit precursor and the oxidizing component of the metastable redox pair. Generally speaking, to be convertible, the metal complex must possess a more positive standard potential than the reducing agent (see Section 3.3), and the plated metal must be active enough in the anodic reducer oxidation to ensure autocatalytic growth.[31] Even non-noble metals such as Al can be deposited under extreme conditions (absence of water and air, aggressive inorganic reducer $LiAlH_4$),[58,59] but the aforementioned criteria result in electroless plating mostly being limited to the late transition metals. With standard reduction potentials between −0.25 V and −0.44 V,[62] Fe,[63] Co,[64,65] and especially Ni[14,18,27,66,67] can be named as the least noble but still regularly plated metals. Protocols are also available for Pd,[37,68] Pt[13,69] and the coinage metals Cu,[70,71] Ag[35,51–56] and Au.[12,19,48,72] For the most part, easily accessible and affordable standard salts such as sulfates, nitrates or chlorides are deployed as metal precursors (*e.g.*, $NiSO_4$, $CuSO_4$, $AgNO_3$, $PdCl_2$). Their role is typically limited to introducing the desired metal ions, but the counter ions can potentially serve as ligands and affect the plating reaction.

Intriguingly, despite clearly fulfilling the criteria of nobility and catalytic prowess, the platinum group metals Ru, Rh, Ir, Os[6] and also Re[73] are only scarcely deposited with electroless plating. Likely, factors such as high complex stability, a plethora of oxidation states and alternative reaction paths pose obstacles towards autocatalytic deposition. For instance, dissolved Ru(III) acetylacetonate was found to completely resist reduction in the excessive presence of $NaBH_4$. Instead, the strong reducer was hydrolyzed by the Ru(III) complex in a homogeneously catalyzed reaction.[74] In electroless plating baths, Re could only be co-deposited with metals which catalyze and promote perrhenate reduction, thus opening the autocatalytic reaction channel.[73] Similar difficulties in related reactions hint at fundamental issues complicating the solution reduction of certain platinum group metals. For instance, Ir electrodeposition is rarely performed and plagued by problems such as low Faradaic efficiency.[75] Only few electroless nanoplating protocols have only been reported for these metals, including Rh[76] and Ir,[77] the latter focusing on the particularly intricate Ir solution chemistry. Further development in this direction is both welcome and challenging. Additional driving force could be provided by employing autoclaves, which would allow one to use hydrogen gas as the primary reducer (likewise to supercritical reactions)[60] and to apply harsher hydrothermal conditions.

Reasonably noble main group metals (*e.g.*, Sn, Pb or Bi) are also candidates for electroless plating, despite their generally lower catalytic activities. These metals are not utilized frequently, and corresponding reactions often suffer from large impurity fractions[78] and employ unusual reducers (*e.g.*, thiourea,[78] Sn(II)).[79] Selective metal deposition can be achieved through carefully balancing the metastable redox pair, as demonstrated in electroless Bi nanoplating.[80]

The reactivity of metal complexes can be tuned by varying their oxidation state and ligand shell. As a rule of thumb, low oxidation states are beneficial because they lessen the electron requirement for reduction and limit the number of potential intermediates (*e.g.*, partially reduced Pt(II) forming aside elemental Pt in a Pt(IV)-based bath).[69] Popular ligands comprise anions of chelating organic acids (*e.g.*, ethylenediaminetetraacetate, citrate, tartrate), but also softer Lewis bases (*e.g.*, ethylenediamine or sulfite), which work well with noble metal ions (*e.g.*, Pd(II)[6] or Au(I)).[48] The complexation strength and steric hindrance of the chosen ligand affect the metal ion reducibility and thus are of key interest for achieving metastable conditions.[33] Ligands often serve multiple roles: They can prevent precipitation (*e.g.*, formation of poorly soluble compounds such as $Ni(OH)_2$ in alkaline baths),[33,66] act as buffers (*e.g.*, ammonia or carboxylic acids),[56] form adsorbates on the deposited metal (*e.g.*, cyanide poisoning Au surfaces in substrate-selective electroless plating),[40] and can even function as reducing agent (*e.g.*, organic amines).[39,81] An interesting example for the latter is sulfite, which is used to stabilize Au(I) ions in electroless formulations, but apparently can also reduce Au(I) complexes (thiosulfate-sulfite based plating baths work in the absence of a conventional reducer).[48]

3.3. Reducing Agent

Standard potentials of typical reducers amount between −1.1 V and −1.4 V,[6] in theory negative enough to reduce all common target metals. This, however, is not observed in experiment, highlighting the importance of looking beyond ideal electrochemical thermodynamics and account for the specific situation at hand. Both the equilibrium potentials and the kinetics of the reduction and oxidation half reactions are markedly affected by numerous factors (*e.g.*, concentration, pH value, temperature, complexation, autocatalytic activity, adsorbates). Typical reducers are stronger in alkaline environment (*e.g.*, hydrazine,[6] tartrate,[54] hypophosphite,[31] formaldehyde).[82] In the case of borohydride and aminoboranes, lower pH values promote reducer loss by solvolysis.[9] Hydroxylamine, hydrazine, and hypophosphite are applicable in acidic bath formulations and helpful when working with base-sensitive substrates.[9,12,47]

Although electroless plating is feasible with a vast range of reducing agents, a privileged set is employed particularly often:

hypophosphite, hydrazine, dimethylaminoborane (DMAB), borohydride and formaldehyde.[6,9] Figure 4 shows a selection of reducers categorized based on the atom type oxidized during the reaction (or, in the case of boron, the atom carrying the actual reducer, negatively polarized hydrogen). These encompass organic compounds (*e.g.*, aldehydes, carbohydrates), salts of inorganic acids (*e.g.*, hypophosphite, sulfite), boron-hydrogen compounds, and compounds with weak nitrogen/oxygen single bonds and a strong tendency to decay into N_2 or O_2 (*e.g.*, hydrazine, hydroxylamine, hydrogen peroxide). Occasionally, reducing metal ions[42,79,83] and sulfur compounds[48] are used as well.

All major reducers are converted under abstraction of hydrogen atoms, which can either recombine to form hydrogen gas or can be further oxidized to protons, releasing additional electrons in the process.[84,85] Metals representing potent (de) hydrogenation catalysts (*e.g.*, Pd, Pt) thus promise efficient autocatalytic deposition and complete reducer oxidation. While the generalized classification of electroless plating as a dehydrogenation reaction suggested by van den Meerakker is an insightful concept integrating many experimental observations,[84] it is not strictly true, since autocatalytic depositions can be realized without hydrogen-bearing reducers.

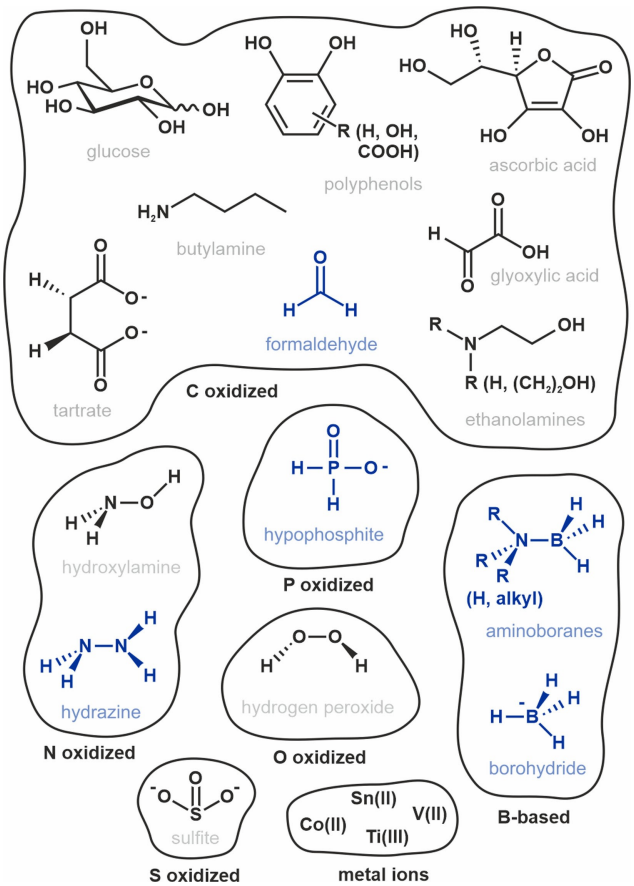

Figure 4. Chemical structures of exemplary reducing agents employed in electroless plating reactions sorted by the oxidized compound part. Standard reducers are highlighted in blue.

Reducers should be selected with the autocatalytic properties of the plated metal and the deposit composition in mind. Ohno *et al.* provide an excellent starting point for identifying reducers which are efficiently oxidized on different metals.[31] Ni and Co work well with hypophosphite, aminoboranes and hydrazine,[27] which is also used for depositing platinum group metals.[6] Coinage metal plating often employs organic reducers, notably formaldehyde,[82,85] but also milder variants such as tartrate,[54] glucose,[35,86] polyphenols,[87] ascorbic[41,88,89] or glyoxylic acid.[90] Due to its extraordinary nobility, gold can even be plated with H_2O_2.[12,91] Whereas carbon- and nitrogen-based reducers yield pure deposits,[6,9,47] phosphorous- and boron-based ones frequently cause heteroatom codeposition, which allows plating Ni–B and Ni–P alloys.[27] Heteroatom inclusion disturbs the deposit lattice, resulting in products of reduced crystallinity, down to semi-amorphous materials and metallic glasses,[27,66,92] albeit the exact nanostructure of such materials often is difficult to resolve and subject to debate.[93] Reducer heteroatoms are not always codeposited, though (*e.g.*, P was found in Re–Ni alloys, but not B).[73] The specific metal chemistry (importantly, the willingness to form borides or phosphides) can be consulted to anticipate inclusion. Due to its natural tendency to create heteroatom-doped and glassy alloys, materials exhibiting interesting functional properties (*e.g.*, favourable reactivity-selectivity profiles in (de) hydrogenations,[93] high oxygen evolution reaction performance),[94] electroless strategies are promising for producing metal catalysts.[95] Amorphous deposits such as Ni–P and Ni–B alloys represent metastable solid solutions and can be transformed into the respective crystalline compounds by heat treatments (*e.g.*, Ni–B into mixtures of Ni and Ni_3B).[96]

Strong reducing agents are highly reactive and thus many a time toxic, carcinogenic and corrosive. From the perspective of green chemistry, electroless plating reactions can exhibit valuable characteristics (availability of harmless reducers, water as solvent, performable at ambient temperatures, high deposition yields attainable). While process-related waste water is an ongoing issue,[9] and it is likely impossible to replace problematic chemicals in all cases (*e.g.*, potent reducers are needed for the less noble metals), electroless nanoplating can benefit from more benign reagents and procedures. For instance, toxic reducers and additives can be replaced,[89,90] and Ni(II) ions can be efficiently plated out of electroless waste water with hypophosphite, a technique suitable for recovering elemental Ni[97] and for creating functional materials alike.[98]

3.4. Additives

Popular additive types include surfactants, stabilizers, accelerators, buffers, and stress reducers.[9,99,100] In nanotechnological applications, shape-directing[19,20] and porogenic agents[101] are expedient. Often, the exact mechanistic impact of additives is poorly understood.[100] Advancements in this area are crucial for moving from the inefficient trial-and-error development and overreliance on tried-and-true approaches, which impair the progress in many nanotechnological fields, towards a more

rational synthesis design.[5,44,102–104] The small concentrations at which certain additives already markedly affect metal deposition highlight the susceptibility of interfacial reactions such as electroless plating to impurities (*e.g.*, plating rate reductions of $>50\,\%$ can be observed at concentrations of 10 μM).[100]

Additives allow adjusting the autocatalytic activity of the deposit, which resembles the controlled poisoning of heterogeneous catalysts for fine-tuning their reactivity (*e.g.*, increasing the hydrogenation selectivity with Lindlar catalysts).[105] Likewise to the former, the blocking of particularly active sites can be central for curtailing overshooting electroless plating reactions. Most bath stabilizers can be divided into four classes (Ref. [9], pp. 34–52):[100] Molecules containing heavy chalcogens (*e.g.*, thiourea or thiosulfate), oxyanions (*e.g.*, AsO_2^- or IO_3^-), heavy metal cations (*e.g.*, Pb^{2+}), and unsaturated organic acids (*e.g.*, maleic acid). Strongly adsorbing anions such as cyanide or iodide can also represent potent stabilizers.[100] In nanomaterials plating, compounds such as halides,[53] citrate[86,106] or 4-mercaptobenzoic acid,[88] which are known to adsorb onto the plated metals, have proven valuable for limiting their deposition,[53,86] for changing the morphology from dense to (nano)particulate coatings,[53,86] and for growing anisotropic nanostructures.[53,88] Considering the large surface area, small crystallite size and defectiveness of such products, it is clear that kinetic control[104] represents a key strategy for plating high-energy products of particular nanotechnological interest.

4-(dimethylamino)pyridine (DMAP) is a rare example of a rationally introduced plating additive. Initially, this molecule was employed as organocatalyst in nucleophilic acyl substitutions.[107] In a first transition to nanotechnology, Gittins and Caruso applied the electron-rich pyridine as a polar capping agent for the spontaneous phase transfer of metal nanoparticles from toluene to water.[108] Later, Gandubert and Lennox showed that the capping is not overly strong: Effective Au nanoparticle stabilization relies on an excess of DMAP and a not too acidic pH to ensure the presence of unprotonated pyridine adsorbates.[109] The Burgess group strengthened the understanding of the pH- and facet-dependent adsorption of DMAP on gold with electrochemical and spectroscopic investigations[110,111] and used it to create branched Au nanoparticles, for which a partial reduction of the highly reactive Au(III) precursor to Au(I) was necessary.[112]

Several of DMAP's characteristics render it an interesting auxiliary reagent for electroless plating:[72] (i) It is water-soluble and thus compatible with the typically aqueous bath chemistry. (ii) It reversibly adsorbs onto metal surfaces with medium strength, modifying the autocatalytic activity while still keeping plating viable. The interaction can be easily tuned by adjusting the pH value and concentration, and after deposition, DMAP can be removed by washing with diluted acids. (iii) The occurrence of facet-selective adsorption indicates potential for shape control.

Like suggested by its adsorption onto Pd and Au nanoparticles,[108] DMAP could be used to design nanoplating reactions for both metals.[37,72] By choosing a Au(I)-DMAP complex as metal precursor, different surfaces could be directly functionalized with Au nanowires by anisotropic, seeded growth.[19] This reaction exemplifies lessons to be learnt from viewing electroless plating and related approaches such as colloidal nanoparticle syntheses[112] from a unified perspective. The fact that DMAP also can be used for electrodepositing anisotropic Au nanostructures further strengthens this point.[113]

Electroless plating contrasts colloidal syntheses in that it does not rely on dedicated capping agents: The deposited nanostructures are growing on surfaces and thus are shielded against aggregation by their immobilization, at least to some extent. One exception is the intermediate case of plating finely dispersed substrates, in which capping agents can be required to prevent clumping.[12] The fact that electroless plating does not call for capping agents likely is advantageous in certain applications (*e.g.*, for realizing high catalytic activity).[114] While this hypothesis has been brought forward in the past,[72] further investigation is required to supply unequivocal experimental evidence. Due to the absence of classical protecting agents in typical bath formulations (*e.g.*, polyvinylpyrrolidone, alkanethiols), one could retroactively apply such compounds to electrolessly plated nanomaterials and compare their catalytic performance and surface chemistry to as-deposited variants.

3.5. Plating Bath Design

A potential heuristic for developing new electroless plating baths starts with a metal source, from which metal complex solutions are derived by adding water and suitable ligands. To each of these, a reducer solution is added, followed by a catalytically active substrate to initiate plating. At each stage, problems can occur: Insoluble precipitates can form when mixing dissolved metal salts with other components, the addition of a too potent reducer can cause homogeneous nucleation, and metal deposition might not proceed even on catalytic surfaces. Such disruptions start optimization loops in which one aims at solving the issue at hand. Stronger or weaker ligands/reducers can be used,[33,80] additives introduced, the reaction conditions changed (*e.g.*, concentration, pH value, temperature, catalyst), and the procedure adapted (*e.g.*, performing kinetically inhibited ligand exchange reactions at elevated temperature before assembling the plating bath,[69,115] or pre-reducing a metal complex to reach a desired oxidation state).[19] Once an operational bath formulation has been established, the impact of selected parameters on the reaction dynamics and the deposit properties can be investigated.

4. Nanomaterials Synthesis

Electroless plating is suitable for producing dispersed nanoobjects, for template-assisted syntheses, and for growing nanostructures or nanoscale films on surfaces.[116] The latter is interesting for directly functionalizing surfaces (avoiding separate nanostructure synthesis, purification, and attachment steps) and can contribute to a good mechanical and electrical connection between substrate and nanostructure. Nanomaterials can also be derived from electrolessly plated structures by

additive, subtractive or converting post-deposition steps, although these options are not dealt with in detail here (*e.g.*, coating plated electrodes with other nanostructures,[98,117] creating nanoporous deposits by chemical etching,[118] or thermally oxidizing plated nanostructures).[71,101]

4.1. Substrate Preparation and Chemistry

Similar to electrodeposition, a proper substrate state is essential for producing high quality materials with electroless plating. Treatments such as degreasing, roughening or oxide removal are routinely applied to facilitate homogeneous metallization and ensure good deposit adhesion.[9] While electroless nanoplating is likewise affected by, *e.g.*, fatty residues, it can experience reduced adhesion issues, because intensely structured substrates can provide efficient mechanical interlocking, and stress build-up is less severe in ultrathin, discontinuous, or even island-like coatings.[119] Adhesion also depends on the substrate-deposit interaction and thus can be improved by tuning the surface chemistry.[120]

It is evident that the earliest reaction stages, which are affected by the still uncovered substrate, are of special relevance for producing defined nanomaterials. A high density of polar groups on the substrate facilitates its wetting and interaction with many reagents (*e.g.*, Sn(II) or Cu(II) ions for seeding).[45,121] As such, substrates can greatly benefit from hydrophilization treatments (*e.g.*, glass with Piranha solution,[55] graphite with *aqua regia*,[45] alumina and polymer template membranes with H_2O_2,[122,123] polymers with chromic acid)[38] and similar interface optimizations (*e.g.*, aminosilanization or similar amine functionalizations,[15,124] polycarboxylate grafting,[121] atmospheric-pressure plasma treatment).[125]

In rare cases, the substrate also guides the deposition through epitaxial growth.[41,126,127] Substrate deterioration due to contact with reactive and corrosive solutions must also be taken into account. Electroless plating and galvanic displacement can proceed simultaneously if the substrate has a more negative standard potential than the metal to be deposited. While this reactivity can form catalytically active immersion deposits (which might be welcome to initiate plating),[128] it can also result in the buildup of corrosion products, uncontrolled chemical attack, and poorly adhering deposits. Chemically sensitive substrates such as cellulose[129] or polycarbonate[66,76] might suffer from degradation, embrittlement, or dissolution during the reaction.

4.2. Seeding

In the majority of cases, the substrate-solution interface must catalyze the electroless plating reaction to reliably initiate metallization. Substrates frequently do not possess sufficient intrinsic activity, which can be amended by decorating them with catalytic seeds. This is commonly realized through three routes (Figure 5): (i) The substrate is rendered reducing (*e.g.*, by attaching Sn(II) ions[45,130–132] or hypophosphite,[95] by absorbing

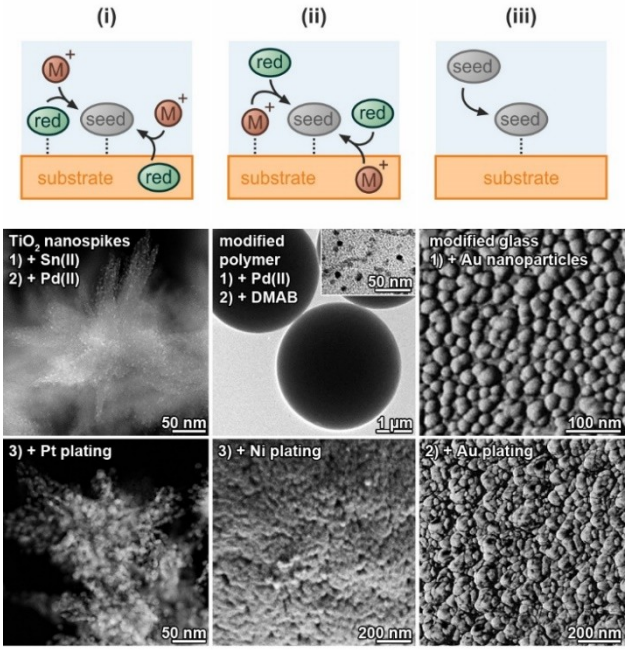

Figure 5. Seeding strategies employed in electroless plating, utilizing metal ions, reducers, and pre-synthesized seeds. Below each strategy, a synthetic example is shown, presenting TEM (i, ii top), SEM (ii bottom) and AFM (iii) images of seeded and plated substrates. (i) Adapted from Ref. [45] with permission; copyright 2019, American Chemical Society, (ii) Adapted from Ref. [124] with permission; copyright 2012, Elsevier. (iii) Adapted from Ref. [140] with permission, copyright 2003, American Chemical Society.

reducers,[119] or by decoration with polydopamine,[133,134] which constitutes a beautiful example of bioinspired surface functionalization).[135] Metal nanoparticles form once such a sensitized substrate is brought into contact with reactive enough metal ions, which can either stem from an activation solution or the plating bath itself. A separate activation step allows one to independently control and tune the seeding and plating conditions,[119,136] while processes are more streamlined if seeds are formed *in situ* upon immersing sensitized substrates into a plating bath.[133] (ii) The aforementioned reaction steps can also be inverted: Metal ions can first be attached to a substrate and then reduced either in the plating bath, a separate solution,[121,124] or with alternative methods such as photoreduction.[137] Anchoring groups for surface complexes can be established, *e.g.*, through molecular self-assembly,[138] polyelectrolyte coatings,[120] or organic functionalization.[124] Alternatively, precursors can be infiltrated into the substrate (*e.g.*, polyimide can be loaded with $Pd(acac)_2$ in supercritical CO_2[139] or hydrolyzed and ion-exchanged with Ag(I)).[137] (iii) Pre-synthesized metal nanoparticles can be bound to the substrate using self-assembled monolayers (SAMs),[28] polycation coatings,[140] or oppositely charged surfaces.[141]

Sn–Pd-based activation strategies represent a standard both in academic research and industry.[9,132] Such reactions are applicable to various substrate materials and can be adapted to produce nanoparticles of other sufficiently noble metals (*e.g.*, Ag,[55] Au).[142] However, they also introduce potentially undesired residues (*e.g.*, oxidized Sn species,[55,132] metallic Sn in

alloyed seeds, such as suggested for Pd),[132] and the chemistry of tin-based sensitization solutions is complex and dynamic.[143]

Seeding reactions are worthwhile syntheses in themselves and should be valued apart from their use as plating pretreatments. With them, surfaces can be decorated with metal nanoparticles in a controlled fashion: The nanoparticle density can be increased by repeating the seeding reaction[95,130,131] or by adapting the reagent concentrations,[119,144] different metals can be introduced,[119,144] and seeds can be ripened to change their shape, size, and distribution.[55] Also, they often are compatible with 3D work pieces, straightforward and quick to perform, and do not require strong protection chemistry. For instance, slightly swollen polymers can be loaded with a reducer, which leaches after the transfer to a metal complex solution, causing nanoparticles to precipitate at the polymer-solution interface.[119,144] This reaction solely works with basic metal salts and reducers (*e.g.*, $AgNO_3$ and DMAB).

Because the seeds initiate the deposit nucleation, their size, uniformity, distribution, and activity decisively impact the onset of metallization. In order to obtain defined nanomaterials, it is thus advisable to mutually optimize the employed seeding and plating reactions.

4.3. Patterning

The activation energy barrier of electroless plating allows one to restrict metal deposition to interfaces promoting the reaction. As such, patterning strategies can be used to selectively coat specific substrate areas. Inversely, specific areas can be blocked to restrict metallization (*e.g.*, with photolithography,[28] soft lithography,[145] simple printing,[121] or by confining the deposition through microfluidic channels).[17,146] For accurate nanoscale patterns, the process resolution is obviously critical, but the structural fidelity can also be obstructed by too large or misplaced deposit particles. If the patterning relies on seeds, they should be active, small, and attached to the chosen substrate areas in a dense, firm, homogeneous and selective fashion. The faithful reproduction of nanoscale features is of great importance for creating miniaturized conductive patterns[28] and template-assisted nanostructure syntheses alike (see Section 4.5).

SAMs[28] and grafted ligands[121] are commonly patterned with lithographic techniques. The Walker group explored an innovative concept for the seedless patterned metallization at the interface of two adjacent, hydrophilic and hydrophobic SAMs, the latter enriching the reducer DMAB, while the former favors metal deposition.[147,148] All reagent classes employed in electroless plating, including the reducing agent,[134] ligand,[149] and catalyst seed,[150] can be applied with (microcontact)[151] printing for patterning purposes.

External stimuli can locally initiate metallization as well. Seed patterns can be created by the photoreduction of sensitive Ag salts,[137] and the reactivity of an electroless Ag plating bath can be restricted so strongly (using $AgNO_3$ as the metal source, no alkaline reagents, and citrate as ligand, adsorbate, and rather weak reducer) that metallization only proceeds *via* plasmon-mediated reduction on Au seeds, which can be spatially controlled with photomasks.[106] Localized heating, which has been implemented, *e.g.*, in the patterned growth of oxide nanostructures,[152] represents an interesting option for electroless plating, albeit the decomposition tendency of overheated plating baths has to be considered.

4.4. Deposition of Nanoparticle Coatings and Nanofilms

Nanoparticle coatings and ultrathin metal films represent routine morphologies for electroless plating (Figure 6). As the deposits typically nucleate at multiple sites, it is natural for a metal film to start as separated nanoparticles (Figure 6A), followed by a percolation stage characterized by growing, merging islands (Figure 6B), which finally transitions into a closed layer (Figure 6C).[55,131,153] The seed distribution and plating time represent straightforward parameters for adjusting the size and density of nanoparticle coatings.[55,154] Increasing the areal density and decreasing the size of seeds reduces the thickness thresholds for percolating and closed films.[140,154,155] In conjunction with smooth, fine-grained deposits, this allows constructing thin films of low roughness.[144] However, the granularity of electroless films makes it challenging to produce extremely thin yet compact coatings. Deposit particles are commonly polydisperse, but it is possible to selectively grow them in a specific shape (see Section 4.6).

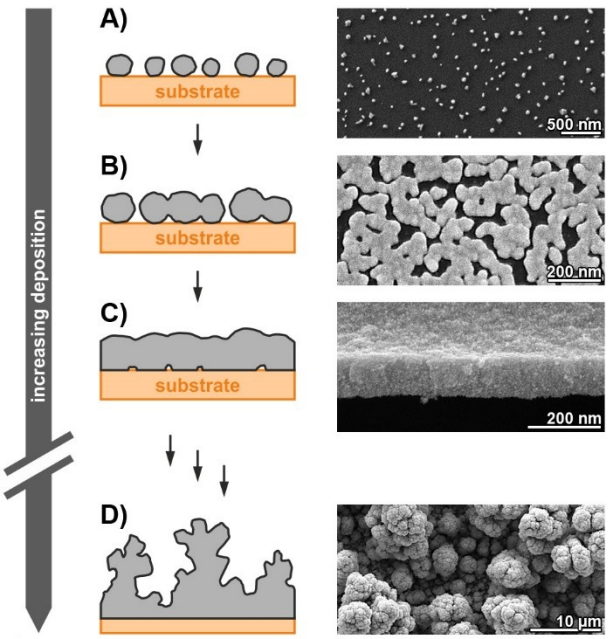

Figure 6. Archetypical morphologies of electrolessly plated metal films with nanoscale features, each complemented by a synthetic example: A) Island-like Ag nanoparticle film on glass; B) percolating Au nanoparticle film on polyvinyl alcohol; C) cross-section of a free-standing, ultrathin Pt film released from its substrate; D) late grow stages of an extremely rough Cu film. SEM images adapted with permission from Ref. [55] (A) (copyright 2019, American Chemical Society), Ref. [119] (B) (copyright 2014 Elsevier), Ref. [144] (C) (copyright 2013, Springer Nature), and Ref. [160] (D) (copyright 2005, Elsevier).

Ultrathin metal deposits can bring classical applications of electroless plating to the nano realm. Ni nanofilms can protect Cu nanotubes and nanowires from oxidation.[71,156] Also, electroless plating has found versatile application in nanoscale electronics research (*e.g.*, for merging crossing nanowires, greatly reducing their contact resistance in transparent conductors,[157] or narrowing the distance between nanogap electrodes),[41,158] and is implemented in flexible and wearable electronics.[134]

Thicker films can also possess nanoscale surface features, which can be superimposed with microscale roughness to create hierarchically structured coatings (Figure 6D). Examples include porous, micrometer-scale waves obtained by wrinkling just percolating Au films,[153] cauliflower-like coatings caused by branching, nodular growth,[159,160] and dendrites formed at high plating rates,[65] akin to electrodeposition. Such materials are interesting, *e.g.*, for surface-enhanced Raman scattering,[153] superhydrophobic coatings,[53,159,161] or heterogeneous catalysis.[160]

4.5. Templated Synthesis of 0D-3D Nanomaterials

Templating represents the perhaps most common strategy for producing metal nanomaterials with electroless plating. It exploits the method's outstanding conformality to define the product morphology, using templates as mold for the deposited metal. The obtained products resemble inverse replica of the original template morphology, whose reproduction quality depends on the nucleation density, the size and shape of the deposit particles, and their nestling against the template surface. Positive nanostructured replica are accessible through dual replication, using the electrolessly plated, optionally reinforced metal as mold for a second material addition step to fill out the void created by removing the original template.[161]

Templates are regularly considered a means to an end and removed after plating, but can also serve diverse functions in the final material. Template matrices can support nanostructures too fragile to endure isolation,[72] liquid template droplets can encapsulate components for later release,[12] and titania templates can offer photocatalytic activity.[162] The presence of easily accessible interfaces on the surface and inside the submicron pores of template membranes greatly facilitates the interaction of plated nanostructures with dissolved chemical species, rendering such membranes interesting platforms for miniaturized flow reactors,[46,77] for expediting the antibody-antigen binding kinetics in immunoassays,[163–165] and for the selective transport of molecules and ions.[166]

Because the metal deposits are formed by merging grains, template-assisted electroless syntheses usually yield polycrystalline materials of rather undefined internal structure, contrasting many colloidal products (compare, *e.g.*, an electrolessly plated, polycrystalline Ag nanowire[131] with a multiply twinned, faceted Ag nanowire of pentagonal cross-section).[5] Though uncommon, single-crystalline products can be realized with template-assisted plating if the deposit nuclei grow undisturbed.[167,168]

While electroless plating is perfectly suited to evenly coat work pieces no matter their structural complexity,[14] surfaces require some degree of accessibility to be homogeneously metallized, and the method struggles with templates possessing expansive inner surfaces connected through narrow and deeply recessed pores. Templates of increasing volumetric surface areas require more metal (and thus more reagents to diffuse from the bulk solution into the template interior) for a homogeneous deposit coverage. Reagent diffusion is noticeably obstructed in small pores acting as bottlenecks, particularly in the mesoscale regime and below.[118,166] The interplay between reagent consumption within a template and diffusive supply from the exterior bath is a typical cause for depletion and reduced plating rates, especially in more convoluted locations. This issue is exacerbated by preferential deposition at exposed areas (*e.g.*, outward facing pore openings),[155] which further narrows diffusion pathways over time. In the worst-case scenario, the pore openings through which the interior surfaces are connected to the bulk solution are completely sealed, preventing any further deposition within the template.[52]

Accordingly, it is compulsory to bolster the deposit conformality when working with demanding templates (*e.g.*, membranes enclosing high aspect ratio nanopores,[72] aerogel monoliths,[169] or mesoporous silica).[170] This can be achieved through various strategies: (i) The plating rate can be reduced to lessen reagent consumption and give natural diffusion more leeway to replenish the solution and maintain roughly constant deposition conditions throughout the template. However, it might be necessary to slow down plating so strongly that metallization proceeds over the course of many hours up to several days,[89,171] which burdens process efficiency. (ii) Convective processes can accelerate solution replenishment in the template. Examples include flushing the plating bath through the template[46,155, 169] and bubble-driven micro-convection in channel-shaped pores caused by gas-releasing reducers.[71,172] (iii) Hierarchical pore systems can be used in which large, continuous pores facilitate reagent transport into crossing nanopores.[54] (iv) Metal nucleation can be tuned so that the ongoing deposition does not block diffusive access to the nanostructure growth front, *e.g.*, by positioning few isolated seeds in a porous template which can grow isotopically,[18] or by linearly growing nanostructures from one side of a porous template to the other.[167] (v) The reducing and oxidizing components can be spatially separated (or consecutively applied)[173] and only allowed to combine and react in the template pores.[118,126,170,172–175] This strategy suppresses mixing of the redox pair in the bulk solution, which alleviates stability issues and facilitates the use of potent reagents. Even if the template pores are filled, plating can still proceed *via* segregated half reactions (in such scenarios, each end of the deposited nanostructures contacts one of the two reagent compartments and acts as anode and cathode, respectively).[174,175]

Optimal conformality also makes demands on the seeding step. The seeds' catalytic activity should surpass that of the plated metal to favor metallization of still uncovered seeds over the growth of already formed deposits, which promotes a high

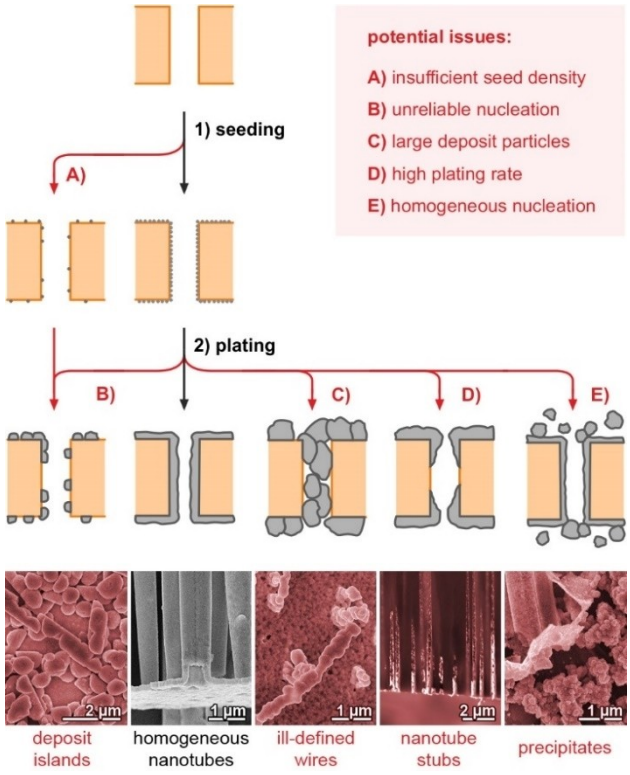

Figure 7. Scheme of potential issues hampering the electroless plating of metal nanotubes in porous template membranes. Each scenario is illustrated with a SEM image showing corresponding metal nanostructures, which have been freed from their templates, with the exception of scenario D) (author's unpublished results).

nucleation density, particularly in difficult to access template areas.[119] *Vice versa*, the autocatalytic activity of the deposit can be lowered by the plating conditions.[176]

Several of the previously discussed problems encountered in template-assisted nanomaterials syntheses are summarized in Figure 7, using metal nanotubes with closed walls as an exemplary target morphology. Depending on the specific scenario, other requirements and synthetic strategies might become relevant. For instance, in order to enhance the diffusion to interior active sites, surface area and mass-normalized catalytic activity of metal nanotubes,[89,177] it can be advantageous to strive for thin, porous tube walls, which likely has to be traded in for a reduced mechanical robustness.

Depending on the template geometry, nanomaterials of arbitrary dimensionality can be plated (Figure 8). In the case of 0D nanomaterials, the difference between seed and template blurs. Dispersed seeds can be enlarged or overgrown by a metal shell to obtain nanoparticles, a strategy the Monnier group pioneers to obtain supported nanoparticle catalysts.[13,49,178–180]

By coating the walls of channel-shaped template pores, nanotubes, nanowires, nanorods and intermediate 1D objects can be created, depending on the conformality, the amount of plated metal and the pore diameter, with narrower pores favoring wire-like morphologies.[54,131] Filling such pores either from well-separated, embedded seed particles[181] or from one side[167] allows depositing nanowires reliably. These approaches requires considerable deposit thicknesses to realize extended nanostructures and thus benefit from fast plating rates, like provided by commercial electroless plating solutions.[167] Common porous templates for plating 1D nanostructures include

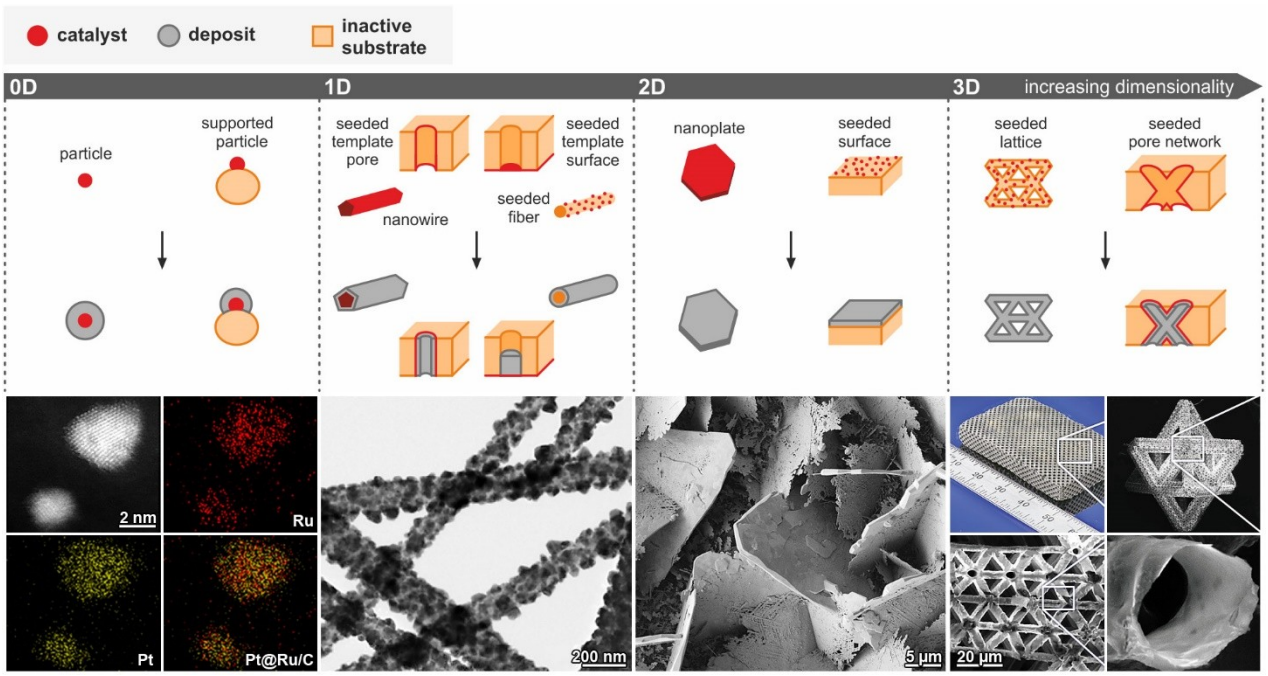

Figure 8. Scheme of template-assisted electroless nanomaterials syntheses, sorted by increasing product dimensionality. Below each category, an example is shown: 0D core-shell nanoparticles; 1D titania nanofibers coated with Ag nanoparticles; 2D Ag nanoplates electrolessly overcoated with Ag, prepared according to Ref. [46]; 3D hierarchical, hollow Ni–P lattice. Material characterization adapted with permission from Ref. [179] (0D; copyright 2015, American Chemical Society), Ref. [162] (1D; copyright 2014, American Chemical Society), and Ref. [14] (3D; copyright 2016, Nature Publishing Group).

track-etched membranes,[54,123,171] nanoporous anodized alumina,[122] and mesoporous silica.[181] Solid 1D templates such as electrospun nanofibers are also employed,[162,182] providing a scalable route towards conducting textiles.[183] Contrary to colloidal, linearly growing nanowires, the complete surface of template fibers can be metallized simultaneously, allowing the fabrication of centimeter-long nanotubes.[184] 1D nanostructures of limitless aspect ratio are invaluable for metal-based transparent conductors,[182,184] which achieve percolation at ultralow coverages through the crossing of continuous, extended, and narrow conduction paths.[185] By combining electroless plating and galvanic displacement steps, multiwalled metal nanotubes can be created from 1D precursors,[186,187] providing a route towards extended nanoscale gaps. Nanowires can be overcoated to obtain core-shell architectures.[156,188] 2D nanostructures include ultrathin films (see section 4.4) and coated nanoplate templates.[46]

Electroless plating can perhaps most impressively demonstrate its conformality in the preparation of 3D nanostructured materials. The most ambitious design I have encountered so far is a lattice structured on multiple length scales, which is solely composed of ~60 nm thick, nanotubular struts. Due to its careful hierarchical design and the nanoscale deposit thickness, this metamaterial transforms the brittle Ni–P alloy it is composed of into an elastic architecture enduring close to 20% tensile strain.[14] Examples of other deliberately constructed 3D nanomaterials include nanotube networks,[54,171,177,189] bichiral plasmonic crystals,[26] and opal-templated nanoshell lattices.[190] Free-standing nanomaterials of high surface area, tailored open porosity and defined structure represent elaborate platforms for electrochemical and catalytic applications.[117,127,171,191]

4.6. Shape-Controlled Electroless Plating

While templating represents a general strategy for synthesizing nanomaterials of comparable, tunable morphology and variable composition, it involves additional processing steps (*e.g.*, template synthesis, modification, removal). Also, it remains restricted in terms of the deposit fine structure: Electrolessly plated nanomaterials typically constitute complicatedly shaped, polycrystalline, rather disordered metal thin films – no less, no more. Considering the value a precise control over the nanoarchitecture has for establishing structure-property relationships and improving material properties, it is very much desirable to empower electroless plating to yield products which possess specific crystal habits, defects, or terminating facets.

This can be achieved by switching from the extrinsic structural control of templates to an intrinsic one: Rather than forcing a growing deposit into shape by blocking space, its structure can be defined by directed growth instead. The latter can be understood as a hybrid approach combining the characteristics of electroless plating and shape-controlled nanoparticle synthesis (Figure 9). Shape-controlled electroless plating reactions provide a facile route for amplifying the surface area of substrates and for directly functionalizing them with defined metal (nano)crystals, making them appealing for interface-

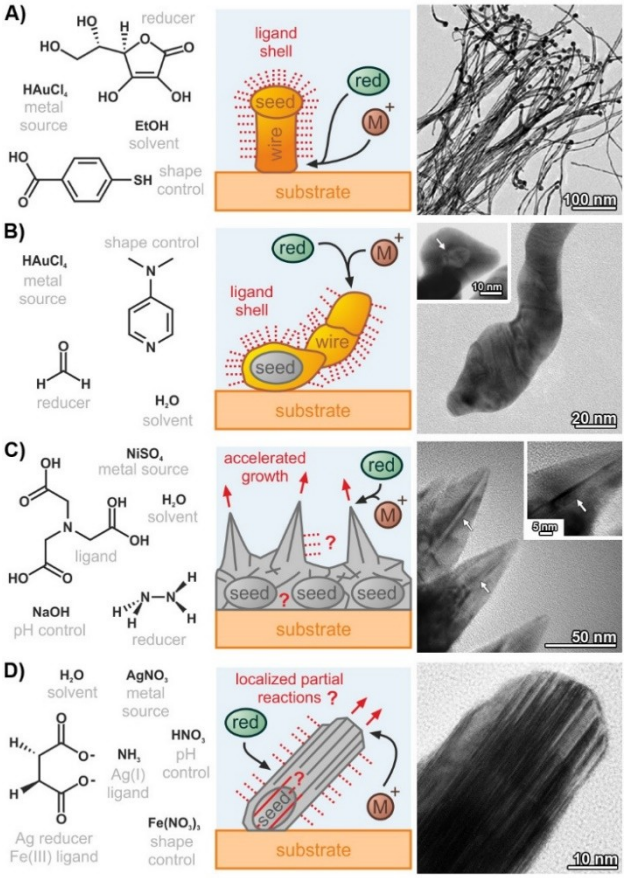

Figure 9. Examples of shape-controlled electroless plating reactions, summarizing the bath components, the proposed growth mechanism and the nanostructure. A) Au nanowires. B) Au nanowires (prepared according to Ref. [19], arrow marks a Pd seed core encapsulated by deposited Au). C) Ni nanospikes (arrows mark twinning). D) Ag nanoplates. TEM images adapted with permission from Ref. [88] (A) (copyright 2013, American Chemical Society), Ref. [67] (C) (copyright 2019, American Chemical Society), and Ref. [46] (D) (copyright 2018, Wiley-VCH). Question marks denote uncertainties regarding the seed-deposit interface, adsorbate formation, or spatial decoupling of the partial reactions.

driven applications.[19,46,192–195] On the other hand, such reactions abandon the universality of templating for the staggering complexity of controlled nanostructure growth. While differently composed but structurally related nanostructures can be straightforwardly created by applying various plating reactions to identical templates,[171] it is nigh impossible to design from scratch a shape-controlled plating bath that selectively deposits a given metal in a specific nanostructure. Finding general plating chemistries for depositing different metals in the form of structurally associated nanocrystals is even more challenging, given the marked element dependence of such reactions.

While shape-controlled electroless plating operates independently from templating, it can be combined with it to produce ever more complex nanomaterials (*e.g.*, applying nickel nanospike plating to template membranes for spiky nanotube networks).[67]

Several reactions yielding shape-controlled metal nanostructure coatings comply with the mechanism of electroless

plating, but are not explicitly named as such. Examples include the seeded growth of Au nanowire films, in which the nanowire surface is protected by mercaptobenzoic acid (Figure 9A). Here, metal deposition is restricted to the wire-substrate interface, pushing the growing nanostructure upwards.[88,196] Single-crystalline Pt nanowires can be deposited from solutions containing chloroplatinic and formic acid as metal precursor and reducer, respectively.[193,194]

Being so far from predictive design, progress in shape-controlled electroless plating will likely be fueled by the discovery of new reactions, detailed mechanistic analysis, and utilizing knowledge from the parent field of colloidal nanoparticle synthesis. Such reactions have several mechanistic requirements: First, random 3D nucleation, which favors polycrystalline, disordered deposits, must be suppressed. The long-range order of the crystal lattice serves as foundation for extending structural motifs beyond atomic distances. Thus, amorphous, isotropically growing deposits must also be avoided.[67] Under these circumstances, the shape of the deposit crystals can be tuned by accelerating or curbing the growth rates in certain crystallographic directions. However, the pronounced symmetry of most metal lattices impedes the formation of highly anisotropic single crystals. Akin to colloidal syntheses,[44,104] this restriction can be overcome by symmetry breaking: Selective nucleation at the nanostructure tips, in conjunction with fast passivation of the sides, enables the self-guided growth of nanowires[19] (Figure 9B), while accelerated deposition at surfacing twin defects allows plating drawn-out shapes such as nanoplates[20,46] or nanospikes[66,67] (Figure 9C, D). Defects can generate and stabilize active sites, such as shown for nanoplate edges[197] or grain boundaries,[198] making such materials valuable for heterogeneous catalysis and site-selective derivatization.[46]

Shape-controlled electroless plating is frequently observed under curtailed growth,[19,20,53,194] which helps limiting uncontrolled nucleation and realizing kinetic products characterized by high aspect ratios, surface areas, and defect densities. By adding increasing amounts of halides[53] or Fe(III) complexes[20] to Ag baths, the plating rate can be continuously reduced, which first results in coarsened deposits (from polycrystalline, dense coatings to micron-sized, faceted particles of seemingly high crystallinity[53] or thick, low aspect ratio plates)[20] and transitions into selective nanoplate formation at low enough values. This observation is in accord with a generalized mechanism proposed for colloidal systems, which convincingly connects the 2D growth of face-centered cubic metals to low driving forces.[199] In a related series of polyol-based Pd nanoparticle syntheses, following a decreasing reaction rate, the products transitioned from single-crystalline over multiply twinned and roundish particles to stacking-fault laden platelets.[200] Likewise, in electroless plating using triethanolamine as a weak and slow reducer, Ag nanoplates could be deposited.[81] Interestingly, in this reaction, a slightly elevated temperature of 30 °C was required to obtain high aspect ratio nanoplates. While rising temperatures accelerate the plating reaction, they also affect other growth-relevant parameters such as diffusion, adsorption, adatom mobility, and (re) crystallization. Thus, even if one aims at metal deposition far from equilibrium to realize highly anisotropic nanostructures, it can be beneficial to operate at (moderately) elevated temperatures.[20,81] Apart from defects, phase engineering is an important aspect of metal nanomaterial design, and metastable crystal structures accessible through colloidal syntheses[201] might also be attainable by autocatalytic deposition. Since unusual phases can offer altered properties and increased reactivity,[201] exploring them in the context of electroless nanoplating appears significant, despite the lack of hitherto reported examples.

In many shape-controlled plating reactions, adsorption plays a major role: Mixed Fe(III)-tartrate-hydroxide complexes were found to adsorb onto the deposit, reducing the growth perpendicular to the basal {111} nanoplate faces with increasing Fe(III) concentration.[20] Chloride could affect Ag nanoplate formation through Ag(I) complexation and oxidative etching (fostered by the reduced standard potential of halogen compounds), but its substoichiometric use in conjunction with an excess of the chelator ethylenediamine the plating bath makes adsorption the most likely cause (due to the low solubility of silver halides, a suitably strong ligand was required to reach chloride concentrations sufficient for shape control).[53] Silver has an exceptionally low stacking fault energy, which promotes the spontaneous formation of planar defects during crystal growth.[202] This could explain the relative abundance of electroless systems for the deposition of 2D silver crystals such as nanoplates and nanobelts.[20,53,81]

Often, the evolution of anisotropic deposit features is not fully understood.[67,192,194] For instance, Au nanospikes could be grown from $HAuCl_4$-hydroxylamine-based baths in the presence of trace amounts of Ag(I), whose role remains unclear.[203] This reaction could share similarities with colloidal Ag–Au systems affected by Ag underpotential deposition, although this rationale was used to explain the tuning of single-crystal habits by changing the relative stability of facets.[102] Spatial decoupling of the oxidation and reduction partial reactions[20,204] and local pH changes induced by selective plating at active nanostructure areas[19] also have been brought forward as potential origins of anisotropy. Thus, a better understanding of the local reaction dynamics would be of great mechanistic value.[44] Nickel nanospike plating was found to depend on the chosen ligand,[67] but the reducer hydrazine itself might constitute the shape-directing agent (simultaneously acting, *e.g.*, as ligand[205] and/or adsorbate), as nanospikes have been found in the absence of dedicated ligands (just using an aqueous solution containing hydrazine, NaOH and $NiSO_4$).[206] Control over the orientation of anisotropic deposits has also been demonstrated (*e.g.*, Ag nanoplates aligning due to epitaxial growth[46] or plasmon-mediated reduction with polarized light).[207]

Intriguingly, electroless plating reactions can be highly shape-selective even without efforts to ensure monodisperse seeds,[19,20,193] contrasting the tendency of colloidal systems to heavily rely on uniform starting points.[5] This behavior could be enabled by dominant metal deposition on particularly active subsets of seeds or nanostructure types,[19] by selective self-seeding, or by positive feedback unifying different emerging

structures into a single growth motif. Generally, the seed-deposit interactions during the early plating stages warrant further investigation.

4.7. Alloy Plating and Multimetallic Nanostructures

Moving from single- to multimetallic nanostructures opens up new dimensions for functionality tuning, offering plentiful motivation for developing corresponding electroless nanoplating reactions (Figure 10). Depending on the coordination, redox and alloying chemistries of the involved metals, solutions containing multiple metal precursors can deposit nanostructures of differing elemental distribution, including fully alloyed, heterobimetallic, core-shell, or gradient-containing variants.[49,208,209] Summaries of established electroless alloy plating protocols represent valuable sources for developing new reactions,[210] testing existing ones in nanotechnological applications, and for guiding systematic studies, which are needed to achieve a better understanding of these particularly intricate reactions.

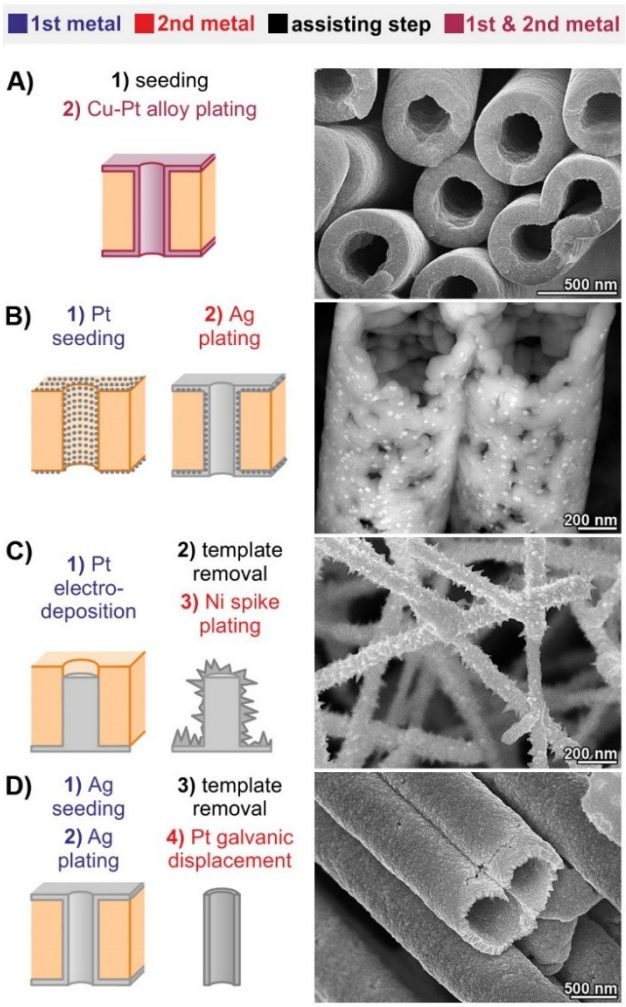

Figure 10. Electroless plating strategies towards bimetallic nanomaterials: A) alloy plating, B) seed implantation, C) consecutive plating, and D) galvanic displacement. Each part outlines the synthesis of an exemplary 1D nanostructure: A) Cu–Pt alloy nanotubes, B) Pt-nanoparticle-dotted Ag nanotubes, C) Pt core Ni nanospike shell nanowires (prepared according to Ref. [195]), D) Ag–Pt alloy nanotubes (prepared according to Ref. [187]). SEM images adapted with permission from Ref. [115] (A) (copyright 2020, The Authors), Ref. [119] (B) (copyright 2014, Elsevier).

The presence of multiple metal precursors aggravates the complexity of electroless plating baths, rendering autocatalytic alloy deposition a challenging endeavor. Similar plating rates must be achieved for all metals to be present as more than trace or dominating components, and their ratio should be adjustable to allow for composition tuning. As the plating potential and kinetics result from the interplaying partial reactions, they cannot be controlled directly (compare, *e.g.*, with the freely adjustable reduction potential in electrodepositions), but rather depend on a multitude of often dynamic factors, including the deposit activity, bath composition, temperature, and pH value. Detrimental interferences between bath components must be avoided (*e.g.*, the ligand for one metal ion could form a poorly soluble compound with another), and simultaneously fulfilling the metastability criterion for several redox pairs is difficult (*i.e.*, realizing sufficient bath stability even if another, more noble and easily reducible metal species is present).

A straightforward solution is to mix compatible plating baths which utilize similar chemicals and operate under similar conditions. This represents the foundation for plating Fe, Ni, Co and their (heteroatom-doped) alloys, which can all be deposited in a comparable fashion with borane- or hypophosphite-based baths.[211,212] The available alloy portfolio can be expanded upon by designing and matching compatible baths, like shown with the deposition of composition-tunable Pd–Pt nanotubes[189] and Ni–Pd–P metallic glasses.[92] Large standard potential differences between involved metals can cause plating rates to differ too strongly to reach a desired alloy composition. Using the more reactive metal in low concentration exacerbates selective bath depletion and deposit inhomogeneity. In such cases, the minority component can be continuously added over time to ensure constant plating conditions and bath stability, like demonstrated in the Ag–Pd[213] and Pt–Cu systems.[49]

One can break down the complexity of electroless plating baths by reducing the number of components, by limiting their interactions, or by overriding their original reactivities. Selectively operating ligands can completely invert the reactivity of metals in alloy systems, enabling the deposition of previously inaccessible element combinations. For instance, cyanide interacts particularly strongly with ionic and elemental Au, resulting in efficient stabilization of Au complexes and poisoning of Au surfaces. In formaldehyde-based Au–Cu plating baths, cyanide was employed to prevent immediate decomposition caused by the high reactivity of Au ions, enabling the deposition of almost fully composition-tunable alloys (a minimum of ~2 at% Cu was required for sufficient autocatalytic activity).[214]

Due the swiftness of most ligand exchange reactions, it is difficult to prevent equilibration between all ligands and metal ions present in alloy plating baths. This issue can be resolved by taking inspiration from the medical application of inert complexes, whose hindered ligand exchange is exploited for

tuning their pharmacokinetic properties: Compounds such as *cis*-diamminedichloroplatinum(II) change their ligand shell so slowly that they can traverse the body mostly unaltered, allowing them to shed their most labile ligands before irreversibly binding to DNA (whose denaturation establishes their use as cytostatic drugs).[215] In materials science, this curious property can be harnessed to decouple the reactivity of different metal precursors employed in the chemical deposition of alloy nanofilms. By adding a series of inert Pt(IV) complexes created in a preceding, thermally activated ligand exchange step to Cu(II)-formaldeyhde solutions, Pt–Cu alloy plating baths are obtained which are metastable with respect to both the coordination of the Pt center and metal reduction (Figure 10A). As such, the Pt speciation (and thus its reduction kinetics) can be adjusted independently from the global solution composition, allowing one to translate the additional synthetic degree of freedom provided by the sluggish ligand exchange to compositional control.[115] Similar schemes should be viable for other inert complexes and codeposited metals.

Heterobimetallic systems can be realized with relative ease by using seeding reactions to implant nanoparticles into electrolessly plated nanostructures[119,136] (Figure 10B). This is interesting, *e.g.*, for achieving functional synergies or efficient noble metal utilization in heterogeneous catalysis.[216] Consecutively plating a different metal on an existing metal nanostructure yields layered products such as core-shell nanotubes,[71] nanowires[156,188,195] (Figure 10C), or nanoparticles.[178,179] By plating bimetallic alloy shells onto catalyst seeds, trimetallic Pd@Pt–Cu nanoparticles could be realized.[49] Conversely, the seed and deposit metals can be unified to create pure metal nanostructures.[136,144]

During electroless plating, galvanic displacement must be considered as a possible side reaction which can leach the seeds[45] or previously deposited metals. This undermines the feasibility of certain metal deposition sequences, but can also serve synthetic purposes: Galvanic displacement can introduce new metals to previously plated nano-objects[187] (Figure 10D), and can accompany electroless plating reactions (*e.g.*, causing elemental mixing in Pd–Pt nanoparticles).[45] The composition and structure of plated multimetallic nanomaterials can also be modified through selective chemical etching.[115,118,187]

4.8. Porous Deposits

Non-compact deposits spontaneously form when nanoparticles repeatedly nucleate without efficiently merging, resulting in more or less loosely aggregated, micro-/mesoporous deposits, such as found for Pt[36] and Rh[76] (Figure 11A). Reducer-associated vivid gas evolution has been suggested to cause narrow, channel-shaped pores in Ni or Co deposits.[217,218] Efforts should be devoted to clearly pinpoint the synthetic requirements for intrinsically porous deposits.

Alternatively, pores can be actively designed and introduced with templates (*e.g.*, block copolymers,[18] nanopatterned photopolymers,[219] liquid crystals,[101] nanoporous gold,[126] mesoporous silica,[170] see Figure 11B) and formed by applying

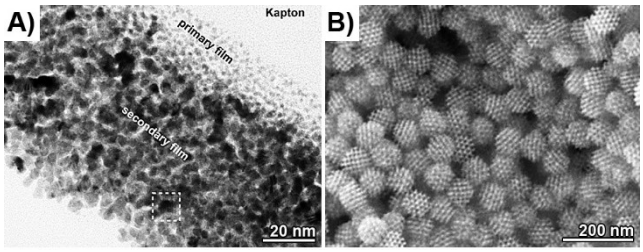

Figure 11. Examples of electrolessly plated nanostructures whose porosity is defined by A) the intrinsic deposit morphology (Pt film) and B) templating (Ag–Au network particles). SEM and TEM images adapted with permission from Ref. [36] (A) (copyright 2010, American Chemical Society) and Ref. [170] (B) (copyright 2018, The Authors).

dealloying and/or galvanic displacement to electrolessly plated nanostructures.[52,186,187] Regardless of their background, small pores can greatly increase the accessible deposit surface area[76,101,218,219] and create confined spaces for chemical reactions.[220]

While dealloying and displacement reactions only have been rarely applied to electrolessly plated nanomaterials, the mechanisms governing the structural and compositional changes should be similar for related precursor materials, regardless of their synthetic origin. Chemical Co leaching during electroless Pt plating onto Co seeds[178] resulted in architectures closely resembling those found for dealloyed Co–Pt and Pt–Cu nanoparticles, which were derived from C-supported Pt nanoparticles by infiltration with metal salts, followed by annealing in hydrogen:[221] Small nanoparticles adopted relatively undisturbed layered structures in which a thin Pt shell protected a less noble core, whereas larger particles exhibited Pt segregation, pitting and pore development, likely driven by Rayleigh instabilities.[221] Galvanic displacement of Ag nanotubes by Au(III) represents a process associated with considerable volume loss (3 Ag atoms are replaced by 1 Au atom, and both metals possess almost identical atomic volumes), which the system accommodates to by developing sponge-like Au walls.[52] This morphology very much resembles that of nanoporous Au obtained by dealloying[222] and galvanic displacement,[223] the former representing the selective removal of an alloy component, the latter a coupled removal-deposition (which also tends to transition through alloy stages).[223] As such, insights established in the field of nanostructure dealloying and displacement are of immediate use when applying such strategies to electrolessly plated precursors. Mechanistically, it is interesting to study systems in more detail which are characterized by overlapping autocatalytic deposition and displacement/etching reactions. Not unlike selective transformations in organic synthesis, finding ways to control and suppress competing reactions can be pivotal to arrive at well-defined inorganic nanomaterials.[224,225]

5. Conclusions

Likewise to its redox-chemical kin, electroless plating represents a pristine example of nanotechnology, building up metallic materials atom by atom. Producing nanostructures with this technique does not require more than dipping substrates into solutions, and terminating the reaction early enough. Luckily, the reality of plating well-defined nanomaterials is much more complicated, providing a huge playground for interdisciplinary scientists. Being able to divert the eye from the method's traditional focus – comparably thick deposits, fast plating rates, inexpensive metals, and a limited cast of applications – opens up exciting new avenues to explore. Despite the age of the field, surprising breakthroughs are still made, such as a mesmerizing Au plating reaction recently reported by the Leach group.[225] Here, epitaxial, single-crystalline nanoscale plating is realized through merely combining $HAuCl_4$ with a high concentration of hydroxide ions, which at the same time arrest the galvanic displacement of the Ag substrate and serve as a green, unexpected reducing agent, releasing oxygen in the process.While optimized plating reactions are convenient to use, they also tend to be difficult to design. The field of electroless nanoplating is broad and evolving, and the chemistry of the plating baths complex. Much of the reactivity is tied to the properties of the metal(s) to be plated (coordination/adsorbate chemistry, redox behavior, catalytic activity, crystal growth, *etc.*), and changing a single parameter usually influences multiple deposit and solution properties at once. This pronounced specificity and interdependence makes it likely that the nanomaterials community will require a large array of complementary nanoplating protocols. A diverse reaction library comprising different metals, alloys and product morphologies would not only represent a useful toolkit for materials engineers, but also facilitate the identification of common mechanistic denominators and generalizable strategies.

As researchers, we should not shy back from this complexity, but embrace it. In-depth mechanistic investigations will be foundational for enhancing both the structural and compositional control of electroless nanoplating, and venturing forth beyond the comparably small set of standard reagents will contribute to unfolding the method's true potential. New insights and directions are also revealed by looking at the method with open eyes. Upon closer inspection, our artificial demarcation lines begin to blur, may the themes be as intimately linked to electroless plating as autocatalytic nanoparticle growth and shape control, or as seemingly disconnected as self-limiting depositions and the unorthodox chemistry of inert platinum complexes.

While the next impactful materials innovation is as unlikely to predict as its enabling technologies, the versatility of electroless nanoplating is evident, and refined protocols represent valuable assets for future materials problems to solve. Being able to strike convincing compromises between material quality and ease of preparation, the method has a distinct potential for helping metal-based nanomaterials to leave the clean rooms and highly specialized laboratories of this world behind and adopt a broader scope, both in academic research and industrial production.

Acknowledgements

Open access funding enabled and organized by Projekt DEAL.

Conflict of Interest

The authors declare no conflict of interest.

Keywords: redox chemistry · nanotechnology · electrocatalysis · transition metals · thin films

[1] R. Jin, C. Zeng, M. Zhou, Y. Chen, *Chem. Rev.* **2016**, *116*, 10346–10413.
[2] H. Mistry, A. S. Varela, S. Kühl, P. Strasser, B. R. Cuenya, *Nat. Rev. Mater.* **2016**, *1*, 16009.
[3] J. A. Liddle, G. M. Gallatin, *ACS Nano* **2016**, *10*, 2995–3014.
[4] A. G. M. da Silva, T. S. Rodrigues, S. J. Haigh, P. H. C. Camargo, *Chem. Commun.* **2017**, *53*, 7135–7148.
[5] a) Y. Xia, K. D. Gilroy, H.-C. Peng, X. Xia, *Angew. Chem. Int. Ed.* **2017**, *65*, 60–95; b) Y. Xia, K. D. Gilroy, H.-C. Peng, X. Xia, *Angew. Chem.* **2017**, *129*, 60–98; *Angew. Chem. Int. Ed.* **2017**, *56*, 60–95.
[6] C. R. K. Rao, D. C. Trivedi, *Coord. Chem. Rev.* **2005**, *249*, 613–631.
[7] K. D. Gilroy, X. Yang, S. Xie, M. Zhao, D. Qin, Y. Xia, *Adv. Mater.* **2018**, *30*, 1706312.
[8] B. J. Plowman, S. K. Bhargava, A. P. O'Mullane, *Analyst* **2011**, *136*, 5107–5119.
[9] G. O. Mallory, J. B. Hajdu, *Electroless Plating: Fundamentals and Applications*, American Electroplaters and Surface Finishers Society, Orlando, Florida, **1990**.
[10] a) H. Niederprüm, *Angew. Chem. Int. Ed.* **1975**, *14*, 614–620; *Angew. Chem.* **1975**, *87*, 652–658; b) H. Niederprüm, *Angew. Chem.* **1975**, *87*, 652–658; *Angew. Chem. Int. Ed.* **1975**, *14*, 614–620.
[11] C. Huang, J. Jiang, M. Lu, L. Sun, E. I. Meletis, Y. Hao, *Nano Lett.* **2009**, *9*, 4297–4301.
[12] K. Stark, J. P. Hitchcok, A. Fiaz, A. L. White, E. A. Baxter, S. Biggs, J. R. McLaughlan, S. Freear, O. J. Cayre, *ACS Appl. Mater. Interfaces* **2019**, *11*, 12272–12282.
[13] K. D. Beard, M. T. Schaal, J. W. Van Zee, J. R. Monnier, *Appl. Catal. B* **2007**, *72*, 262–271.
[14] X. Zheng, W. Smith, J. Jackson, B. Moran, H. Cui, D. Chen, J. Ye, N. Fang, N. Rodriguez, T. Weisgraber, C. M. Spadaccini, *Nat. Mater.* **2016**, *15*, 1100–1106.
[15] Y. Fang, V. W. Chen, Y. Cai, J. D. Berrigan, S. R. Marder, J. W. Perry, K. H. Sandhage, *Adv. Funct. Mater.* **2012**, *22*, 2550–2559.
[16] J. Cai, M. Lan, D. Zhang, W. Zhang, *Appl. Surf. Sci.* **2012**, *258*, 8769–8774.
[17] J. Xu, X. Li, Y. Zhong, J. Qi, Z. Wang, Z. Chai, W. Li, C. Jing, Y. Cheng, *Adv. Mater.* **2018**, *3*, 1800372.
[18] K.-C. Yang, C.-T. Yao, L.-Y. Huang, J.-C. Tsai, W.-S. Hung, H.-Y. Hsueh, R.-M. Ho, *NPG Asia Mater.* **2019**, *11*, 9.
[19] F. Muench, S. Schaefer, L. Hagelüken, L. Molina-Luna, M. Duerrschnabel, H.-J. Kleebe, J. Brötz, A. Vaskevich, I. Rubinstein, W. Ensinger, *ACS Appl. Mater. Interfaces* **2017**, *9*, 31142–31152.
[20] F. Muench, A. Vaskevich, R. Popovitz-Biro, T. Bendikov, Y. Feldman, I. Rubinstein, *Electrochim. Acta* **2018**, *264*, 233–243.
[21] Y. Shacham-Diamand, T. Osaka, Y. Okinaka, A. Sugiyama, V. Dubin, *Microelectron. Eng.* **2015**, *132*, 35–45.
[22] A. Brenner, *NASF Surface Technology White Papers* **2018**, *82*, 9–12.
[23] C. R. Shipley, Jr., *NASF Surface Technology White Papers* **2018**, *82*, 13–24.
[24] A. Brenner, G. Riddell, *J. Res. Natl. Bur. Stand.* **1946**, *37*, 31–34 (RP1725).
[25] A. Wurtz, C. R. Hebd, *Acad. Sci.* **1844**, *18*, 702–704.
[26] A. Radke, T. Gissibl, T. Klotzbücher, P. V. Braun, H. Giessen, *Adv. Mater.* **2011**, *23*, 3018–3021.

[27] J. Sudagar, J. Lian, W. Sha, *J. Alloys Compd.* **2013**, *571*, 183–204.
[28] D. Zabetakis, W. J. Dressick, *ACS Appl. Mater. Interfaces* **2009**, *1*, 4–25.
[29] I. Ohno, *Mater. Sci. Eng. A* **1991**, *146*, 33–49.
[30] P. Bindra, J. Roldan, *J. Appl. Electrochem.* **1987**, *17*, 1254–1266.
[31] I. Ohno, O. Wakabayashi, S. Haruyama, *J. Electrochem. Soc.* **1985**, *132*, 2323–2330.
[32] Y. Onabuta, M. Kunimoto, H. Nakai, T. Homma, *Electrochim. Acta* **2019**, *307*, 536–542.
[33] T. M. Gill, J. Zhao, E. J. W. Berenschot, N. Tas, X. Zheng, *ACS Appl. Mater. Interfaces* **2018**, *10*, 22834–22840.
[34] N. T. K. Thanh, N. Maclean, S. Mahiddine, *Chem. Rev.* **2014**, *114*, 7610–7630.
[35] Q. Meng, K. Qin, L. Ma, C. He, E. Liu, F. He, C. Shi, Q. Li, J. Li, N. Zhao, *ACS Appl. Mater. Interfaces* **2017**, *9*, 30832–30839.
[36] K. P. Pernstich, M. Schenker, F. Weibel, A. Rossi, W. R. Caseri, *ACS Appl. Mater. Interfaces* **2010**, *2*, 639–643.
[37] F. Muench, M. Oezaslan, I. Svoboda, W. Ensinger, *Mater. Res. Express* **2015**, *2*, 105010.
[38] J. Li, Y. Wang, G. Xiang, H. Liu, J. He, *Adv. Mater.* **2019**, *4*, 1800529.
[39] K. Kim, H. S. Kim, H. K. Park, *Langmuir* **2006**, *22*, 8083–8088.
[40] C. D. Iacovangelo, K. P. Zarnoch, *J. Electrochem. Soc.* **1991**, *138*, 983–988.
[41] Y. Y. Choi, A. Kwon, Y. Majima, *Appl. Phys. Express* **2019**, *12*, 125003.
[42] D. Wu, D. J. Solanki, J. L. Ramirez, W. Yang, A. Joi, Y. Dordi, N. Dole, S. R. Brankovic, *Langmuir* **2018**, *34*, 11384–11394.
[43] T.-H. Yang, H.-C. Peng, S. Zhou, C.-T. Lee, S. Bao, Y.-H. Lee, J.-M. Wu, Y. Xia, *Nano Lett.* **2017**, *17*, 334–340.
[44] T.-H. Yang, S. Zhou, K. D. Gilroy, L. Figueroa-Cosme, Y.-H. Lee, J.-M. Wu, Y. Xia, *Proc. Natl. Acad. Sci. USA* **2017**, *114*, 13619–13624.
[45] F. Muench, G. A. El-Nagar, T. Tichter, A. Zintler, U. Kunz, L. Molina-Luna, V. Sikolenko, C. Pasquini, I. Lauermann, C. Roth, *ACS Appl. Mater. Interfaces* **2019**, *11*, 43081–43092.
[46] F. Muench, R. Popovitz-Biro, T. Bendikov, Y. Feldman, B. Hecker, M. Oezaslan, I. Rubinstein, A. Vaskevich, *Adv. Mater.* **2018**, *30*, 1805179.
[47] B. D. Baker, *Surf. Technol.* **1981**, *12*, 77–88.
[48] Y. Okinaka, M. Hoshino, *Gold Bull.* **1998**, *31*, 3–13.
[49] G. Tate, A. Kenvin, W. Diao, J. R. Monnier, *Catal. Today* **2019**, *334*, 113–121.
[50] X. Su, X. Li, C. Y. A. Ong, T. S. Herng, Y. Wang, E. Peng, J. Ding, *Adv. Sci.* **2019**, *6*, 1801670.
[51] K. Lomakin, S. Herold, L. Ringel, J. Ringel, D. Simon, M. Sippel, A. Sion, M. Vossiek, K. Helmreich, G. Gold, *IEEE Trans. Compon. Packag. Technol.* **2019**, *9*, 2476–2481.
[52] F. Muench, M. Rauber, C. Stegmann, S. Lauterbach, U. Kunz, H.-J. Kleebe, W. Ensinger, *Nanotechnology* **2011**, *22*, 415602.
[53] F. Muench, B. Juretzka, S. Narayan, A. Radetinac, S. Flege, S. Schaefer, R. W. Stark, W. Ensinger, *New J. Chem.* **2015**, *39*, 6803–6812.
[54] F. Muench, E.-M. Felix, M. Rauber, S. Schaefer, M. Antoni, U. Kunz, H.-J. Kleebe, C. Trautmann, W. Ensinger, *Electrochim. Acta* **2016**, *202*, 47–54.
[55] F. Muench, A. Solomonov, T. Bendikov, L. Molina-Luna, I. Rubinstein, A. Vaskevich, *ACS Appl. Bio Mater.* **2019**, *2*, 856–864.
[56] C. N. Grabill, D. Freppon, M. Hettinger, S. M. Kuebler, *Appl. Surf. Sci.* **2019**, *466*, 230–243.
[57] B. H. Lipshutz, F. Gallou, S. Handa, *ACS Sustainable Chem. Eng.* **2016**, *4*, 5838–5849.
[58] a) H. M. Lee, S.-Y. Choi, A. Jung, S. H. Ko, *Angew. Chem. Int. Ed.* **2013**, *52*, 7718–7723; *Angew. Chem.* **2013**, *125*, 7872–7877; b) H. M. Lee, S.-Y. Choi, A. Jung, S. H. Ko, *Angew. Chem.* **2013**, *125*, 7872–7877; *Angew. Chem. Int. Ed.* **2013**, *52*, 7718–7723.
[59] N. Koura, H. Nagase, A. Sato, S. Kumakura, K. Takeuchi, K. Ui, T. Tsuda, C. K. Loong, *J. Electrochem. Soc.* **2008**, *155*, D155–157.
[60] A. H. Romang, J. J. Watkins, *Chem. Rev.* **2010**, *110*, 459–478.
[61] T. S. Rodrigues, M. Zhao, T.-H. Yang, K. D. Gilroy, A. G. M. da Silva, P. H. C. Camargo, Y. Xia, *Chem. Eur. J.* **2018**, *24*, 16944–16963.
[62] D. R. Lide, *CRC Handbook of Chemistry and Physics, 87th edition*, CRC Press, Florida, **2006**.
[63] J. Blickensderfer, P. Altemare, K.-O. Thiel, H.-J. Schreier, R. Akolkar, *J. Electrochem. Soc.* **2014**, *161*, D495-D498.
[64] P. Yang, X. Zhao, Y. Liu, Y. Gu, *J. Phys. Chem. C* **2017**, *121*, 8557–8568.
[65] S. S. Djokić, *J. Electrochem. Soc.* **1997**, *144*, 2358–2363.
[66] F. Muench, M. Oezaslan, M. Rauber, S. Kaserer, A. Fuchs, E. Mankel, J. Brötz, P. Strasser, C. Roth, W. Ensinger, *J. Power Sources* **2013**, *222*, 243–252.
[67] T. Boettcher, S. Schaefer, M. Antoni, T. Stohr, U. Kunz, M. Dürrschnabel, L. Molina-Luna, W. Ensinger, F. Muench, *Langmuir* **2019**, *35*, 4246–4253.
[68] S. Yu, U. Welp, L. Z. Hua, A. Rydh, W. K. Kwok, H. H. Wang, *Chem. Mater.* **2005**, *17*, 3445–3450.
[69] F. Muench, S. Kaserer, U. Kunz, I. Svoboda, J. Brötz, S. Lauterbach, H.-J. Kleebe, C. Roth, W. Ensinger, *J. Mater. Chem.* **2011**, *21*, 6286–6291.
[70] J. E. Graves, M. E. A. Bowker, A. Summer, A. Greenwood, C. Ponce de León, F. C. Walsh, *Electrochem. Commun.* **2018**, *87*, 58–62.
[71] F. Muench, L. Sun, T. Kottakkat, M. Antoni, S. Schaefer, U. Kunz, L. Molina-Luna, M. Duerrschnabel, H.-J. Kleebe, S. Ayata, C. Roth, W. Ensinger, *ACS Appl. Mater. Interfaces* **2017**, *9*, 771–781.
[72] F. Muench, U. Kunz, C. Neetzel, S. Lauterbach, H.-J. Kleebe, W. Ensinger, *Langmuir* **2011**, *27*, 430–435.
[73] A. Duhin, A. Inberg, N. Eliaz, E. Gileadi, *Electrochim. Acta* **2011**, *56*, 9637–9643.
[74] E. Keçeli, S. Özkar, *J. Mol. Catal. A* **2008**, *286*, 87–91.
[75] J. Näther, F. Köster, R. Freudenberger, C. Schöberl, T. Lampke, *Iop. Conf. Ser. Mater. Sci. Eng.* **2017**, *181*, 012041.
[76] F. Muench, C. Neetzel, S. Kaserer, J. Brötz, J.-C. Jaud, Z. Zhao-Karger, S. Lauterbach, H.-J. Kleebe, C. Roth, W. Ensinger, *J. Mater. Chem.* **2012**, *22*, 12784–12791.
[77] M. C. Scheuerlein, F. Muench, U. Kunz, T. Hellmann, J. P. Hofmann, W. Ensinger, *ChemElectroChem* **2020**, *7*, 3496–3507.
[78] V. R. Nagarajan, P. R. Kharel, S. K. Putatunda, G. Lawes, *Mater. Sci. Eng. B* **2008**, *151*, 191–194.
[79] E. Uchida, K. Tanaka, M. Okada, T. Tsuruoka, K. Akamatsu, H. Nawafune, *Trans. Mater. Res. Soc. Jpn.* **2014**, *39*, 47–51.
[80] M. C. Scheuerlein, W. Ensinger, *RSC Adv.* **2021**, 11, 8636–8642.
[81] Z. Yi, X. Xu, Q. Fang, Y. Wang, X. Li, X. Tan, J. Luo, X. Jiang, W. Wu, Y. Yi, Y. Tang, *Appl. Phys. A* **2014**, *114*, 485–493.
[82] M. de Leo, F. C. Pereira, L. M. Moretto, P. Scopece, S. Polizzi, P. Ugo, *Chem. Mater.* **2007**, *19*, 5955–5964.
[83] E. Norkus, A. Vaškelis, A. Jagminienė, L. Tamašauskaitė-Tamašiūnaitė, *J. Appl. Electrochem.* **2001**, *31*, 1061–1066.
[84] J. E. A. M. van den Meerakker, *J. Appl. Electrochem.* **1981**, *11*, 395–400.
[85] J. E. A. M. van den Meerakker, *J. Appl. Electrochem.* **1981**, *11*, 387–393.
[86] J. E. Chen, Q. Wang, K. R. Shull, J. J. Richards, *J. Colloid Interface Sci.* **2020**, *576*, 376–384.
[87] Y. Ohtani, A. Horiuchi, A. Yamaguchi, K. Oyaizu, M. Yuasa, *J. Electrochem. Soc.* **2006**, *153*, C63-C66.
[88] J. He, Y. Wang, Y. Feng, X. Qi, Z. Zeng, Q. Liu, W. S. Teo, C. L. Gan, H. Zhang, H. Chen, *ACS Nano* **2013**, *7*, 2733–2740.
[89] E.-M. Felix, F. Muench, W. Ensinger, *RSC Adv.* **2014**, *4*, 24504–24510.
[90] J. H. Byeon, J.-W. Kim, *J. Colloid Interface Sci.* **2010**, *348*, 649–653.
[91] K. Jajcevic, K. Sugihara, *J. Phys. Chem. B* **2020**, *124*, 5761–5769.
[92] A. Shibata, Y. Imamura, M. Sone, C. Ishiyama, Y. Higo, *Thin Solid Films* **2009**, *517*, 1935–1938.
[93] J. Geng, D. A. Jefferson, B. F. G. Johnson, *Chem. Eur. J.* **2009**, *15*, 1134–1143.
[94] J. Masa, C. Andronescu, H. Antoni, I. Sinev, S. Seisel, K. Elumeeva, S. Barwe, S. Marti-Sanchez, J. Arbiol, B. R. Cuenya, M. Muhler, W. Schuhmann, *ChemElectroChem* **2019**, *6*, 235–240.
[95] K. C. Poon, D. C. L. Tan, T. D. T. Vo, B. Khezri, H. Su, R. D. Webster, H. Sato, *J. Am. Chem. Soc.* **2014**, *136*, 5217–5220.
[96] S. Arai, Y. Imoto, Y. Suzuki, M. Endo, *Carbon* **2011**, *49*, 1484–1490.
[97] K. Horikawa, I. Hirasawa, *Korean J. Chem. Eng.* **2000**, *17*, 629–632.
[98] Y. Zhu, S. Yuan, D. Bao, Y. Yin, H. Zhong, X. Zhang, J. Yan, Q. Jiang, *Adv. Mater.* **2017**, *29*, 1603719.
[99] N. Nwosu, A. Davidson, C. Hindle, M. Barker, *Ind. Eng. Chem. Res.* **2012**, *51*, 5635–5644.
[100] J. Bieliński, K. Kamiński, *Surf. Coat. Technol.* **1987**, *31*, 223–233.
[101] S.-M. Bak, K.-H. Kim, C.-W. Lee, K.-B. Kim, *J. Mater. Chem.* **2011**, *21*, 1984–1990.
[102] M. L. Personick, C. A. Mirkin, *J. Am. Chem. Soc.* **2013**, *135*, 18238–18247.
[103] K.-S. Choi, *Dalton Trans.* **2008**, 5432–5438, https://pubs.rsc.org/en/content/articlelanding/2008/dt/b807848c#!divAbstract
[104] a) Y. Wang, J. He, C. Liu, W. H. Chong, H. Chen, *Angew. Chem. Int. Ed.* **2015**, *54*, 2022–2051; *Angew. Chem.* **2015**, *127*, 2046–2079; b) Y. Wang, J. He, C. Liu, W. H. Chong, H. Chen, *Angew. Chem.* **2015**, *127*, 2046–2079; *Angew. Chem. Int. Ed.* **2015**, *54*, 2022–2051.
[105] G. Vilé, N. Almora-Barrois, S. Mitchell, N. López, J. Pérez-Ramírez, *Chem. Eur. J.* **2014**, *20*, 5926–5937.
[106] H. Yoshikawa, A. Hironou, Z. Shen, E. Tamiya, *ACS Appl. Mater. Interfaces* **2016**, *8*, 23932–23940.

[107] a) B. Neises, W. Steglich, *Angew. Chem. Int. Ed.* **1978**, *17*, 522–524; *Angew. Chem.* **1978**, *90*, 556–557; b) B. Neises, W. Steglich, *Angew. Chem. Int. Ed.* **1978**, *90*, 556–557.
[108] a) D. I. Gittins, F. Caruso, *Angew. Chem. Int. Ed.* **2001**, *40*, 3001–3004; *Angew. Chem.* **2001**, *113*, 3089–3092; b) D. I. Gittins, F. Caruso, *Angew. Chem. Int. Ed.* **2001**, *113*, 3089–3092.
[109] V. J. Gandubert, R. B. Lennox, *Langmuir* **2005**, *21*, 6532–6539.
[110] S. M. Rosendahl, B. R. Danger, J. P. Vivek, I. J. Burgess, *Langmuir* **2009**, *25*, 2241–2247.
[111] J. P. Vivek, I. J. Burgess, *Electrochim. Acta* **2013**, *88*, 688–696.
[112] B. R. Danger, D. Fan, J. P. Vivek, I. J. Burgess, *ACS Nano* **2012**, *6*, 11018–11026.
[113] S. Simon, T. I. Olumorin, B. Guo, I. J. Burgess, *J. Phys. Chem. C* **2016**, *120*, 26150–26158.
[114] Z. Niu, Y. Li, *Chem. Mater.* **2014**, *26*, 72–83.
[115] T. Stohr, J. Brötz, M. Oezaslan, F. Muench, *Chem. Eur. J.* **2020**, *26*, 3030–3033.
[116] M. A. Lim, D. H. Kim, C.-O. Park, Y. W. Lee, S. W. Han, Z. Li, R. S. Williams, I. Park, *ACS Nano* **2012**, *6*, 598–608.
[117] K. M. Amin, F. Muench, U. Kunz, W. Ensinger, *J. Colloid Interface Sci.* **2021**, *591*, 384–395.
[118] Y. Ding, J. Erlebacher, *J. Am. Chem. Soc.* **2003**, *125*, 7772–7773.
[119] F. Muench, A. Eils, M. E. Toimil-Molares, U. H. Hossain, A. Radetinac, C. Stegmann, U. Kunz, S. Lauterbach, H.-J. Kleebe, W. Ensinger, *Surf. Coat. Technol.* **2014**, *242*, 100–108.
[120] T. Tamai, M. Watanabe, Y. Kobayashi, J. Kobata, Y. Nakahara, S. Yahima, *Colloids Surf. A* **2019**, *575*, 230–236.
[121] A. Garcia, J. Polesel-Maris, P. Viel, S. Palacin, T. Berthelot, *Adv. Funct. Mater.* **2011**, *21*, 2096–2102.
[122] L. Velleman, J.-L. Bruneel, F. Guillaume, D. Losic, J. G. Shapter, *Phys. Chem. Chem. Phys.* **2011**, *13*, 19587–19593.
[123] I. V. Korolkov, D. B. Borgekov, A. A. Mashentseva, O. Güven, A. B. Atici, A. L. Kozlovskiy, M. V. Zdorovets, *Chem. Pap.* **2017**, *71*, 2353–2358.
[124] I. Halaciuga, J. I. Njagi, K. Redford, D. V. Goia, *J. Colloid Interface Sci.* **2012**, *383*, 215–221.
[125] M. Šimor, J. Ráhel, M. Černák, Y. Imahori, M. Štefečka, M. Kando, *Surf. Coat. Technol.* **2003**, *172*, 1–6.
[126] a) Y. Ding, A. Mathur, M. Chen, J. Erlebacher, *Angew. Chem. Int. Ed.* **2005**, *44*, 4002–4006; *Angew. Chem.* **2005**, *117*, 4070–4074; b) Y. Ding, A. Mathur, M. Chen, J. Erlebacher, *Angew. Chem.* **2005**, *117*, 4070–4074; *Angew. Chem. Int. Ed.* **2005**, *44*, 4002–4006.
[127] Y. Ding, M. Chen, J. Erlebacher, *J. Am. Chem. Soc.* **2004**, *126*, 6876–6877.
[128] J. I. Njagi, C. M. Netzband, D. V. Goia, *J. Colloid Interface Sci.* **2017**, *488*, 72–78.
[129] Z. Al-Maqdasi, A. Hajlane, A. Renbi, Y. Ouarga, S. S. Chouhan, R. Joffe, *Fibers* **2019**, *7*, 38.
[130] F. Muench, M. Oezaslan, T. Seidl, S. Lauterbach, P. Strasser, H.-J. Kleebe, W. Ensinger, *Appl. Phys. A* **2011**, *105*, 847–854.
[131] F. Muench, U. Kunz, H. F. Wardenga, H.-J. Kleebe, W. Ensinger, *Langmuir* **2014**, *30*, 10878–10885.
[132] X. Wei, D. K. Roper, *J. Electrochem. Soc.* **2014**, *161*, D235-D242.
[133] G. Mondin, F. M. Wisser, A. Leifert, N. Mohamed-Noriega, J. Grothe, S. Dörfler, S. Kaskel, *J. Colloid Interface Sci.* **2013**, *411*, 187–193.
[134] Y. Mao, M. Zhu, W. Wang, D. Yu, *Soft Matter* **2018**, *14*, 1260–1269.
[135] J. H. Ryu, P. B. Messersmith, H. Lee, *ACS Appl. Mater. Interfaces* **2018**, *10*, 7523–7540.
[136] F. Muench, L. Hussein, T. Stohr, U. Kunz, S. Ayata, I. Gärtner, H.-J. Kleebe, W. Ensinger, *Colloids Surf. A* **2016**, *508*, 197–204.
[137] J. Marques-Hueso, T. D. A. Jones, D. E. Watson, A. Ryspayeva, M. N. Esfahani, M. P. Shuttleworth, R. A. Harris, R. W. Kay, M. P. Y. Desmulliez, *Adv. Funct. Mater.* **2018**, *28*, 1704451.
[138] N. M. K. K. Arachchige, P. C. Chambers, A. M. Taylor, Z. L. Highland, J. C. Garno, *ACS Appl. Nano Mater.* **2019**, *2*, 2193–2203.
[139] T.-F. M. Chang, C.-C. Wang, C.-Y. Yen, S.-H. Chen, C.-Y. Chen, M. Sone, *Microelectron. Eng.* **2016**, *153*, 1–4.
[140] S. Hrapovic, Y. Liu, G. Enright, F. Bensebaa, J. H. T. Luong, *Langmuir* **2003**, *19*, 3958–3965.
[141] S. H. Kim, J. A. Jackson, J. S. Oakdale, J.-B. Forien, J. M. Lenhardt, J.-H. Yoo, S. J. Shin, X. Lepró, B. D. Moran, C. M. Aracne-Ruddle, T. F. Baumann, O. S. Jones, J. Biener, *Chem. Commun.* **2018**, *54*, 10463–10466.
[142] Z. Zhang, C. Shao, P. Zou, P. Zhang, M. Zhang, J. Mu, Z. Guo, X. Li, C. Wang, Y. Liu, *Chem. Commun.* **2011**, *47*, 3906–3908.
[143] J. Przyłuski, M. Kasparzak, J. Bieliński, *Surf. Coat. Technol.* **1987**, *31*, 203–211.
[144] F. Muench, S. Bohn, M. Rauber, T. Seidl, A. Radetinac, U. Kunz, S. Lauterbach, H.-J. Kleebe, C. Tratumann, W. Ensinger, *Appl. Phys. A* **2014**, *116*, 287–294.
[145] G. Mondin, B. Schumm, J. Fritsch, R. Hensel, J. Grothe, S. Kaskel, *Mater. Chem. Phys.* **2013**, *137*, 884–891.
[146] E. D. Goluch, K. A. Shaikh, K. Ryu, J. Chen, J. Engel, C. Liu, *Appl. Phys. Lett.* **2004**, *85*, 3629–3631.
[147] Z. Shi, A. V. Walker, *Langmuir* **2011**, *27*, 11292–11295.
[148] A. A. Ellsworth, A. V. Walker, *Langmuir* **2016**, *32*, 2668–2674.
[149] Y. Chang, C. Yang, X.-Y. Zheng, D.-Y. Wang, Z.-G. Yang, *ACS Appl. Mater. Interfaces* **2014**, *6*, 768–772.
[150] D. Zabetakis, W. J. Dressick, *ACS Appl. Mater. Interfaces* **2012**, *4*, 2358–2368.
[151] V. Tjong, L. Wu, P. M. Moran, *Langmuir* **2006**, *22*, 2430–2432.
[152] C. Y. Jin, J. Yun, J. Kim, D. Yang, D. H. Kim, J. H. Ahn, K.-C. Lee, I. Park, *Nanoscale* **2014**, *6*, 14428–14432.
[153] C. M. Gabardo, R. C. Adams-McGavin, B. C. Fung, E. J. Mahoney, Q. Fang, L. Soleymani, *Sci. Rep.* **2017**, *7*, 42543.
[154] K. R. Brown, L. A. Lyon, A. P. Fox, B. D. Reiss, M. J. Natan, *Chem. Mater.* **2000**, *12*, 314–323.
[155] R. J. Gilliam, S. J. Thorpe, D. W. Kirk, *J. Appl. Electrochem.* **2007**, *37*, 233–239.
[156] I. E. Stewart, A. R. Rathmell, L. Yan, S. Ye, P. F. Flowers, W. You, B. J. Wiley, *Nanoscale* **2014**, *6*, 5980–5988.
[157] C.-J. Ni, F. C.-N. Hong, *RSC Adv.* **2014**, *4*, 40330–40338.
[158] V. M. Serdio, V. Y. Azuma, S. Takeshita, T. Muraki, T. Teranishi, Y. Majima, *Nanoscale* **2012**, *22*, 7161–7167.
[159] H. Ogihara, T. Katayama, T. Saji, *J. Mater. Chem.* **2011**, *21*, 14890–14896.
[160] E. Norkus, A. Vaškelis, J. Jačiauskienė, I. Stalnionienė, G. Stalnionis, *Electrochim. Acta* **2006**, *51*, 3495–3499.
[161] H.-X. Huang, X. Wang, *Mater. Today Commun.* **2019**, *19*, 487–494.
[162] Y. Zhao, L. Sun, M. Xi, Q. Feng, C. Jiang, H. Fong, *ACS Appl. Mater. Interfaces* **2014**, *6*, 5759–5767.
[163] M. A. Penn, D. M. Drake, J. D. Driskell, *Anal. Chem.* **2013**, *85*, 8609–8617.
[164] B. Y. Kim, C. B. Swearingen, J. A. Ho, E. V. Romanova, P. W. Bohn, J. V. Sweedler, *J. Am. Chem. Soc.* **2007**, *129*, 7620–7626.
[165] R. Chen, X. Du, Y. Cui, X. Zhang, Q. Ge, J. Dong, X. Zhao, *Small* **2020**, *16*, 2002801.
[166] C. R. Martin, M. Nishizawa, K. Jirage, M. Kang, *J. Phys. Chem. B* **2001**, *105*, 1925–1934.
[167] M. Barbic, J. J. Mock, D. R. Smith, S. Schultz, *J. Appl. Phys.* **2002**, *91*, 9341–9345.
[168] S.-H. Zhang, Z.-X. Xie, Z.-Y. Jiang, X. Xu, J. Xiang, R.-B. Huang, L.-S. Zheng, *Chem. Commun.* **2004**, 1106–1107, https://pubs.rsc.org/en/content/articlelanding/2004/CC/B315931K#!divAbstract.
[169] M. Schestakow, F. Muench, C. Reimuth, L. Ratke, W. Ensinger, *Appl. Phys. Lett.* **2016**, *108*, 213108.
[170] J. Fang, L. Zhang, J. Li, L. Lu, C. Ma, S. Cheng, Z. Li, Q. Xiong, H. You, *Nat. Commun.* **2018**, *9*, 521.
[171] F. Muench, D. M. De Carolis, E.-M. Felix, J. Brötz, U. Kunz, H.-J. Kleebe, S. Ayata, C. Trautmann, W. Ensinger, *ChemPlusChem* **2015**, *80*, 1448–1456.
[172] X.-Z. Li, K.-L. Wu, Y. Ye, X.-W. Wei, *Nanoscale* **2013**, *5*, 3648–3653.
[173] Y. Yan, A. I. Radu, W. Rao, H. Wang, G. Chen, K. Weber, D. Wang, D. Cialla-May, J. Popp, P. Schaaf, *Chem. Mater.* **2016**, *28*, 7673–7682.
[174] C. Koenigsmann, A. C. Santulli, E. Scutter, S. S. Wong, *ACS Nano* **2011**, *5*, 5460–5466.
[175] M. Wood, B. Zhang, *ACS Nano* **2015**, *9*, 2454–2464.
[176] H. Matsubara, T. Yonekawa, Y. Ishino, N. Saito, H. Nishiyama, Y. Inoue, *Electrochim. Acta* **2006**, *52*, 402–407.
[177] T. Walbert, M. Antoni, F. Muench, T. Späth, W. Ensinger, *ChemElectroChem* **2018**, *5*, 1087–1097.
[178] K. D. Beard, D. Borrelli, A. M. Cramer, D. Blom, J. W. Van Zee, J. R. Monnier, *ACS Nano* **2009**, *3*, 2841–2853.
[179] W. Diao, J. M. M. Tengco, J. R. Regalbuto, J. R. Monnier, *ACS Catal.* **2015**, *5*, 5123–5134.
[180] W. Diao, J. M. M. Tengco, A. M. Gaffney, J. R. Regalbuto, J. R. Monnier, J. Spivey, Y.-F. Han, D. Shekhawat, *Catalysis: Volume 32*, Royal Society of Chemistry, London, United Kingdom, **2020**, 116–150.
[181] N. Petkov, N. Stock, T. Bein, *J. Phys. Chem. B* **2005**, *109*, 10737–10743.
[182] P–C. Hsu, D. Kong, S. Wang, H. Wang, A. J. Welch, H. Wu, Y. Cui, *J. Am. Chem. Soc.* **2014**, *136*, 10593–10596.

[183] Y. Chen, Z. Wang, R. Xu, W. Wang, D. Yu, *Chem. Eng. J.* **2020**, *394*, 124960.
[184] S.-Y. Min, Y. Lee, S. H. Kim, C. Park, T.-W. Lee, *ACS Nano* **2017**, *11*, 3681–3689.
[185] S. Ye, A. R. Rathmell, Z. Chen, I. E. Stewart, B. J. Wiley, *Adv. Mater.* **2014**, *26*, 6670–6687.
[186] Y. Sun, Y. Xia, *Adv. Mater.* **2004**, *16*, 264–268.
[187] S. Schaefer, F. Muench, E. Mankel, A. Fuchs, J. Brötz, U. Kunz, W. Ensinger, *NANO* **2015**, *10*, 1550085.
[188] S. Cherevko, X. Xing, C.-H. Chung, *Electrochim. Acta* **2011**, *56*, 5771–5775.
[189] T. Stohr, A. Fischer, F. Muench, M. Antoni, S. Wollstadt, C. Lohaus, U. Kunz, O. Clemens, A. Klein, W. Ensinger, *ChemElectroChem* **2020**, *7*, 855–864.
[190] W. Dong, H. Dong, Z. Wang, P. Zhan, Z. Yu, X. Zhao, Y. Zhu, N. Ming, *Adv. Mater.* **2006**, *18*, 755–759.
[191] R. Xu, L. Du, D. Adekoya, G. Zhang, S. Zhang, S. Sun, Y. Lei, *Adv. Energy Mater.* **2020**, 2001537.
[192] K. M. Metz, K.-Y. Tse, S. E. Baker, E. C. Landis, R. J. Hamers, *Chem. Mater.* **2006**, *18*, 5398–5400.
[193] P. Daubinger, J. Kieninger, T. Unmüssig, G. A. Urban, *Phys. Chem. Chem. Phys.* **2014**, *16*, 8392–8399.
[194] S. Sun, D. Yang, D. Villers, G. Zhang, E. Sacher, J.-P. Dodelet, *Adv. Mater.* **2008**, *20*, 571–574.
[195] X. Zhao, F. Muench, S. Schaefer, J. Brötz, M. Duerrschnabel, L. Molina-Luna, H.-J. Kleebe, S. Liu, J. Tan, W. Ensinger, *Electrochem. Commun.* **2016**, *65*, 39–43.
[196] Y. Wang, J. He, S. Yu, H. Chen, *Small* **2016**, *12*, 930–938.
[197] N. M. Andoy, X. Zhou, E. Choudhary, H. Shen, G. Liu, P. Chen, *J. Am. Chem. Soc.* **2013**, *135*, 1845–1852.
[198] R. G. Mariano, K. McKelvey, H. S. White, M. W. Kanan, *Science* **2017**, *358*, 1187–1192.
[199] B. Viswanath, P. Kundu, B. Mukherjee, N. Ravishankar, *Nanotechnology* **2008**, *19*, 195603.
[200] Y. Wang, H.-C. Peng, J. Liu, C. Z. Huang, Y. Xia, *Nano Lett.* **2015**, *15*, 1445–1450.
[201] Y. Chen, Z. Lai, X. Zhang, Z. Fan, Q. He, C. Tan, H. Zhang, *Nature Rev. Chem.* **2020**, *4*, 243–256.
[202] T. Tan, S. Zhang, J. Wang, Y. Zheng, H. Lai, J. Liu, F. Qin, C. Wang, *Nanoscale* **2021**, *13*, 195–205.
[203] B. Guo, G. Han, M. Li, S. Zhao, *Thin Solid Films* **2010**, *518*, 3228–3233.
[204] J. M. Köhler, A. Knauer, *Appl. Sci.* **2018**, *8*, 1343.
[205] V. Genova, L. Paglia, F. Marra, C. Bartuli, G. Pulci, *Surf. Coat. Technol.* **2019**, *357*, 595–603.
[206] Z. An, S. Pan, J. Zhang, *J. Phys. Chem. C* **2009**, *113*, 1346–1351.
[207] B.-B. Xu, L. Wang, Z.-C. Ma, R. Zhang, Q.-D. Chen, C. Lv, B. Han, X.-Z. Xiao, X.-L. Zhang, K. Ueno, H. Misawa, H.-B. Sun, *ACS Nano* **2014**, *8*, 6682–6692.
[208] N. Ortiz, R. G. Weiner, S. E. Skrabalak, *ACS Nano* **2014**, *8*, 12461–12467.
[209] D. Liang, P. Rajput, J. Zegenhagen, G. Zangari, *ChemElectroChem* **2014**, *1*, 787–792.
[210] I. Ohno, M. Schlesinger, M. Paunovic, *Modern Electroplating, Fifth Edition*, John Wiley & Sons, Inc., Hoboken, New Jersey, **2010**, pp. 499–506.
[211] K. Lee, J. Lee, B. M. Jung, B. Park, T. Kim, S. B. Lee, *Appl. Surf. Sci.* **2019**, *478*, 733–736.
[212] J. F. Rohan, D. P. Casey, B. M. Ahern, F. M. F. Rhen, S. Roy, D. Fleming, S. E. Lawrence, *Electrochem. Commun.* **2008**, *10*, 1419–1422.
[213] G. Zen, L. Shi, Y. Liu, Y. Zhang, Y. Sun, *Int. J. Hydrogen Energy* **2014**, *39*, 4427–4436.
[214] A. Molenaar, *J. Electrochem. Soc.* **1985**, *129*, 1917–1921.
[215] J. Reedijk, *Platinum Met. Rev.* **2008**, *52*, 2–11.
[216] S. Schaefer, E.-M. Felix, F. Muench, M. Antoni, C. Lohaus, J. Brötz, U. Kunz, I. Gärtner, W. Ensinger, *RSC Adv.* **2016**, *6*, 70033–70039.
[217] W. Hao, R. Wu, R. Zhang, Y. Ha, Z. Chen, L. Wang, Y. Yang, X. Ma, D. Sun, F. Fang, Y. Guo, *Adv. Energy Mater.* **2018**, *8*, 1801372.
[218] Z. Wu, M. Zhang, S. Ge, Z. Zhang, W. Li, K. Tao, *J. Mater. Chem.* **2005**, *15*, 4928–4933.
[219] H. Park, C. Ahn, H. Jo, M. Choi, D. S. Kim, D. K. Kim, S. Jeon, H. Choe, *Mater. Lett.* **2014**, *129*, 174–177.
[220] H. Abe, J. Liu, K. Ariga, *Mater. Today* **2016**, *19*, 12–18.
[221] M. Oezaslan, M. Heggen, P. Strasser, *J. Am. Chem. Soc.* **2012**, *134*, 514–524.
[222] I. McCue, E. Benn, B. Gaskey, J. Erlebacher, *Annu. Rev. Mater. Res.* **2016**, *46*, 263–286.
[223] Y. Sun, Y. Xia, *J. Am. Chem. Soc.* **2004**, *126*, 3892–3901.
[224] Y. Wu, X. Sun, Y. Yang, J. Li, Y. Zhang, D. Qin, *Acc. Chem. Res.* **2017**, *50*, 1774–1784.
[225] S. V. Grayli, X. Zhang, F. C. MacNab, S. Kamal, D. Star, G. W. Leach, *ACS Nano* **2020**, *14*, 7581–7592.

Manuscript received: March 3, 2021
Revised manuscript received: April 30, 2021
Accepted manuscript online: May 4, 2021